

# Sparse semiparametric canonical correlation analysis for data of mixed types

Grace Yoon, Raymond J. Carroll and Irina Gaynanova\*

Department of Statistics, Texas A&M University  
3143 TAMU, College Station, TX 77843

## Abstract

Canonical correlation analysis investigates linear relationships between two sets of variables, but often works poorly on modern data sets due to high-dimensionality and mixed data types (continuous/binary/zero-inflated). We propose a new approach for sparse canonical correlation analysis of mixed data types that does not require explicit parametric assumptions. Our main contribution is the use of truncated latent Gaussian copula to model the data with excess zeroes, which allows us to derive a rank-based estimator of latent correlation matrix without the estimation of marginal transformation functions. The resulting semiparametric sparse canonical correlation analysis method works well in high-dimensional settings as demonstrated via numerical studies, and application to the analysis of association between gene expression and micro RNA data of breast cancer patients.

**Keywords:** BIC; Gaussian copula model; Kendall's  $\tau$ ; Latent correlation matrix; Truncated continuous variable; Zero-inflated data.

## 1 Introduction

Canonical correlation analysis investigates linear associations between two sets of variables, and is widely used in various fields including biomedical sciences, imaging and genomics ([Chi et al., 2013](#); [Hardoon et al., 2004](#); [Safo et al., 2018](#)). However, sample canonical correlation analysis often performs poorly due to two main challenges: high-dimensionality and non-normality of the data.

In high-dimensional settings, sample canonical correlation analysis is known to overfit the data due to singularity of sample covariance matrices ([Guo et al., 2016](#); [Hardoon et al., 2004](#)). Additional regularization is often used to address this challenge. [González et al. \(2008\)](#) focus on ridge regularization of sample covariance matrices to avoid singularity, while more recent methods focus on sparsity regularization of canonical vectors ([Chi et al., 2013](#); [Cruz-Cano and Lee, 2014](#); [Parkhomenko et al., 2009](#); [Safo et al., 2018](#); [Wilms and Croux, 2015](#); [Witten et al., 2009](#)). At the same time, with the advancement in technology, it is common to collect data of different types. For example, the Cancer Genome Atlas Project contains matched data of mixed types such as gene expression (continuous), mutation (binary) and micro RNA (count) data. While regularized

---

\*Corresponding author. E-mail: [irinag@stat.tamu.edu](mailto:irinag@stat.tamu.edu)

canonical correlation methods work well for Gaussian data, they still are based on sample covariance matrix, and therefore are not appropriate for the analysis in the presence of binary data or data with excess zero values.

Several approaches have been proposed to address the non-normality of the data. There are completely nonparametric approaches such as kernel canonical correlation analysis (Hardoon et al., 2004). Alternatively, there are parametric approaches building upon a probabilistic interpretation of Bach and Jordan (2005). For example, Zoh et al. (2016) develop probabilistic canonical correlation analysis for count data by exploring natural parameter for Poisson distribution. More recently, Agniel and Cai (2017) utilize a normal semiparametric transformation model for the analysis of mixed types of variables; however, the method requires estimation of marginal transformation functions via nonparametric maximum likelihood.

In summary, a significant progress has been made in developing regularized variants of sample canonical correlation analysis that work well in high-dimensional settings. However, these approaches are not suited for mixed data types. At the same time, several methods have been proposed to account for non-normality of the data, however are not designed for high-dimensional settings. More importantly, to our knowledge none of the existing methods explicitly address the case of zero-inflated measurements, which, for example, is common for micro RNA and microbiome abundance data.

To bridge this major gap, we propose a semiparametric approach for sparse canonical correlation analysis, which allows us to handle high-dimensional data of mixed types via a common latent Gaussian copula framework. Our work has three main contributions.

First, we model the zeros in the data as observed due to truncation of underlying latent continuous variable, and define a corresponding truncated Gaussian copula model. We derive explicit formulas for the bridge functions that connect the Kendall’s  $\tau$  of observed data to the latent correlation matrix for different combinations of data types, and use these formulas to construct a rank-based estimator of the latent correlation matrix for the mixed (continuous/binary/truncated) data. Fan et al. (2017) use bridge function approach in the context of graphical models, however the authors do not consider the truncated variable type. The latter requires derivation of new bridge functions, and those derivations are considerably more involved than corresponding derivations for the continuous/binary case. The significant advantage of the bridge function technique is that it allows us to estimate the latent correlation structure of Gaussian copula without estimating marginal transformation functions, in contrast to Agniel and Cai (2017).

Secondly, we use the derived rank-based estimator instead of sample correlation matrix within the sparse canonical correlation analysis framework that is motivated by Chi et al. (2013) and Wilms and Croux (2015). This allows us to take into account the dataset-specific correlation structure in addition to cross-correlation structure. In contrast, Parkhomenko et al. (2009) and Witten et al. (2009) model the variables within each data set as uncorrelated. We develop an efficient optimization algorithm to solve the corresponding problem.

Finally, we propose two types of Bayesian Information Criterion (BIC) for tuning parameter selection, which leads to significant computational saving compared to commonly used cross-validation and permutation techniques (Witten and Tibshirani, 2009). Wilms and Croux (2015) also use BIC in the canonical correlation analysis context, however only one criterion is proposed. Two criteria originate from BIC formulations for Gaussian linear models depending on whether the case of known or unknown error variance is considered. We found that both are competitive in our numerical studies, however one criterion works best for variable selection, whereas the other works

best for prediction.

## 2 Background

### 2.1 Canonical correlation analysis

In this section we review both the classical canonical correlation analysis, and its sparse alternatives. Given two random vectors  $\mathbf{X}_1 \in \mathbb{R}^{p_1}$  and  $\mathbf{X}_2 \in \mathbb{R}^{p_2}$ , let  $\Sigma_1 = \text{cov}(\mathbf{X}_1)$ ,  $\Sigma_2 = \text{cov}(\mathbf{X}_2)$  and  $\Sigma_{12} = \text{cov}(\mathbf{X}_1, \mathbf{X}_2)$ . Population canonical correlation analysis (Hotelling, 1936) seeks linear combinations  $w_1^\top \mathbf{X}_1$  and  $w_2^\top \mathbf{X}_2$  with maximal correlation, that is

$$\underset{w_1, w_2}{\text{maximize}} \left\{ w_1^\top \Sigma_{12} w_2 \right\} \quad \text{subject to} \quad w_1^\top \Sigma_1 w_1 = 1, \quad w_2^\top \Sigma_2 w_2 = 1. \quad (1)$$

Problem (1) has a closed form solution via the singular value decomposition of  $\Sigma_1^{-1/2} \Sigma_{12} \Sigma_2^{-1/2}$ . Given the first pair of singular vectors  $(u, v)$ , the solutions to (1) can be expressed as  $w_1 = \Sigma_1^{-1/2} u$  and  $w_2 = \Sigma_2^{-1/2} v$ .

The sample canonical correlation analysis replaces  $\Sigma_1$ ,  $\Sigma_2$  and  $\Sigma_{12}$  in (1) by corresponding sample covariance matrices  $S_1$ ,  $S_2$  and  $S_{12}$ . In high-dimensional settings when sample size is small compared to the number of variables,  $S_1$  and  $S_2$  are singular, thus leading to non-uniqueness of solution and poor performance due to overfitting. A common approach to circumvent this challenge is to consider sparse regularization of  $w_1$  and  $w_2$  via the addition of a  $\ell_1$  penalty in the objective function of (1) (Chi et al., 2013; Parkhomenko et al., 2009; Wilms and Croux, 2015; Witten et al., 2009). The sparse canonical correlation analysis is then formulated as

$$\underset{w_1, w_2}{\text{maximize}} \left\{ w_1^\top S_{12} w_2 - \lambda_1 \|w_1\|_1 - \lambda_2 \|w_2\|_1 \right\} \quad \text{subject to} \quad w_1^\top S_1 w_1 \leq 1, \quad w_2^\top S_2 w_2 \leq 1. \quad (2)$$

In addition to  $\ell_1$  penalties, the equality constraints in (1) are replaced with inequality constraints which define convex sets. This generalization is possible since nonzero solutions to (2) satisfy the constraints with equality, see Proposition 1 below.

While problem (2) works well in high-dimensional settings, it still relies on sample covariance matrices, and therefore is not well-suited for skewed or non-continuous data, such as binary or zero-inflated. We next review the Gaussian copula models that we propose to use to address these challenges.

### 2.2 Latent Gaussian copula model for mixed data

In this section we review the Gaussian copula model in Liu et al. (2009), and its extension to mixed (continuous/binary) data in Fan et al. (2017).

**Definition 1** (Gaussian copula model). *A random vector  $\mathbf{X} = (X_1, \dots, X_p)^\top$  satisfies a Gaussian copula model if there exists a set of monotonically increasing transformations  $f = (f_j)_{j=1}^p$  satisfying  $f(\mathbf{X}) = \{f_1(X_1), \dots, f_p(X_p)\}^\top \sim \mathcal{N}_p(0, \Sigma)$  with  $\Sigma_{jj} = 1$ . We denote  $\mathbf{X} \sim \text{NPN}(0, \Sigma, f)$ .*

**Definition 2** (Latent Gaussian copula model for mixed data). *Let  $\mathbf{X}_1 \in \mathbb{R}^{p_1}$  be continuous and  $\mathbf{X}_2 \in \mathbb{R}^{p_2}$  be binary random vectors with  $\mathbf{X} = (\mathbf{X}_1, \mathbf{X}_2)$ . Then  $\mathbf{X}$  satisfies the latent Gaussian copula model if there exists a  $p_2$ -dimensional random vector  $\mathbf{U}_2 = (U_{p_1+1}, \dots, U_{p_1+p_2})^\top$  such that*

$\mathbf{U} := (\mathbf{X}_1, \mathbf{U}_2) \sim \text{NPN}(0, \Sigma, f)$  and  $X_j = I(U_j > C_j)$  for all  $j = p_1 + 1, \dots, p_1 + p_2$ , where  $I(\cdot)$  is the indicator function and  $\mathbf{C} = (C_1, \dots, C_p)$  is a vector of constants. We denote  $\mathbf{X} \sim \text{LNPN}(0, \Sigma, f, \mathbf{C})$ , where  $\Sigma$  is the latent correlation matrix.

Fan et al. (2017) consider the problem of estimating  $\Sigma$  for the latent Gaussian copula model based on the Kendall's  $\tau$ . Given the observed data  $(X_{j1}, X_{k1}), \dots, (X_{jn}, X_{kn})$  for variables  $X_j$  and  $X_k$ , Kendall's  $\tau$  is defined as

$$\hat{\tau}_{jk} = 2\{n(n-1)\}^{1/2} \sum_{1 \leq i < i' \leq n} \text{sign}(X_{ji} - X_{ji'}) \text{sign}(X_{ki} - X_{ki'}).$$

Since  $\hat{\tau}_{jk}$  is invariant under monotone transformation of the data, it is well-suited to capture associations in copula models. Let  $\tau_{jk} = \mathbb{E}(\hat{\tau}_{jk})$  be the population Kendall's  $\tau$ . The latent correlation matrix  $\Sigma$  can be connected to Kendall's  $\tau$  via the so-called bridge function  $F$  such that  $\Sigma_{jk} = F^{-1}(\tau_{jk})$  for all variables  $j$  and  $k$ . Fan et al. (2017) derive an explicit form of the bridge function for continuous, binary and mixed (continuous/binary) variable pairs, which allows them to estimate the latent correlation matrix via the method of moments. We summarize these results below.

**Theorem 1** (Fan et al. (2017)). *Let  $\mathbf{X} = (\mathbf{X}_1, \mathbf{X}_2) \sim \text{LNPN}(0, \Sigma, f, \mathbf{C})$  with  $p_1$ -dimensional continuous  $\mathbf{X}_1$  and  $p_2$ -dimensional binary  $\mathbf{X}_2$ . The rank-based estimator of  $\Sigma$  is given by the symmetric matrix  $\hat{R}$  with  $\hat{R}_{jj} = 1$  and  $\hat{R}_{jk} = \hat{R}_{kj} = F_{jk}^{-1}(\hat{\tau}_{jk})$ , where for  $t \in (0, 1)$ ,*

$$F_{jk}(t) = \begin{cases} 2 \sin^{-1}(t)/\pi & \text{if } 1 \leq j < k \leq p_1; \\ 2 \{\Phi_2(\Delta_j, \Delta_k, t) - \Phi(\Delta_j)\Phi(\Delta_k)\} & \text{if } p_1 + 1 \leq j < k \leq p_1 + p_2; \\ 4\Phi_2(\Delta_j, 0, t/\sqrt{2}) - 2\Phi(\Delta_j) & \text{if } 1 \leq j \leq p_1, p_1 + 1 \leq k \leq p_1 + p_2. \end{cases}$$

Here  $\Delta_j = f_j(C_j)$ ,  $\Phi(\cdot)$  is the cdf of the standard normal distribution, and  $\Phi_2(\cdot, \cdot, t)$  is the cdf of the standard bivariate normal distribution with correlation  $t$

**Remark 1.** Since  $\Delta_j = f_j(C_j)$  is unknown in practice, Fan et al. (2017) propose to use plug-in estimator from the moment equation  $\mathbb{E}(X_{ij}) = 1 - \Phi(\Delta_j)$  leading to  $\hat{\Delta}_j = \Phi^{-1}(1 - \bar{X}_j)$ , where  $\bar{X}_j = \sum_{i=1}^n X_{ji}$ .

Fan et al. (2017) use these results in the context of Gaussian graphical models, and replace the sample covariance matrix with rank-based estimator  $\hat{R}$ , which allows to use Gaussian models with skewed continuous and binary data. However, Fan et al. (2017) do not consider the case of zero-inflated data, which requires formulation of a new model, and subsequently derivation of new bridge functions.

## 3 Methodology

### 3.1 Truncated latent Gaussian copula model

Our goal is to model the zero-inflated data through latent Gaussian copula models. Two motivating examples are micro RNA and microbiome data, where it is common to encounter large number of zero counts. In both examples it is reasonable to model on assumption that zeros are observed due

to truncation of underlying latent continuous variables. More generally, one can think of zeroes as representing the measurement error due to truncation of values below a certain positive threshold. This intuition leads us to consider the following model.

**Definition 3** (Truncated latent Gaussian copula model). *A random vector  $\mathbf{X} = (X_1, \dots, X_d)^\top$  satisfies the truncated Gaussian copula model if there exists a  $d$ -dimensional random vector  $\mathbf{U} = (U_1, \dots, U_d)^\top \sim \text{NPN}(0, \Sigma, f)$  such that*

$$X_j = I(U_j > C_j)U_j \quad (j = 1, \dots, d),$$

where  $I(\cdot)$  is the indicator function and  $\mathbf{C} = (C_1, \dots, C_d)$  is a vector of positive constants. We denote  $X \sim \text{TLNPN}(0, \Sigma, f, \mathbf{C})$ , where  $\Sigma$  is the latent correlation matrix.

The methodology in [Fan et al. \(2017\)](#) allows them to estimate the latent correlation matrix in the presence of mixed continuous and binary data. Our Definition 3 adds a third type, which we denote as *truncated* for short. To construct a rank-based estimator for  $\Sigma$  as in Theorem 1 in the presence of truncated variables, below we derive an explicit form of the bridge function for all possible combinations of the data types (continuous/binary/truncated). Throughout, we use  $\Phi(\cdot)$  for the cdf of a standard normal distribution and  $\Phi_d(\cdot \dots \cdot; \Sigma_d)$  for the cdf of a standard  $d$ -variate normal distribution with correlation matrix  $\Sigma_d$ . All the proofs are deferred to Appendix A.

**Theorem 2.** *Let  $X_j$  be truncated and  $X_k$  be binary. Then  $\mathbb{E}(\hat{\tau}_{jk}) = F(\Sigma_{jk}; \Delta_j, \Delta_k)$ , where*

$$F(\Sigma_{jk}; \Delta_j, \Delta_k) = 2\{1 - \Phi(\Delta_j)\}\Phi(\Delta_k) - 2\Phi_3(-\Delta_j, \Delta_k, 0; \Sigma_{3a}) - 2\Phi_3(-\Delta_j, \Delta_k, 0; \Sigma_{3b}),$$

$$\Delta_j = f_j(C_j), \Delta_k = f_k(C_k),$$

$$\Sigma_{3a} = \begin{pmatrix} 1 & -\Sigma_{jk} & 1/\sqrt{2} \\ -\Sigma_{jk} & 1 & -\Sigma_{jk}/\sqrt{2} \\ 1/\sqrt{2} & -\Sigma_{jk}/\sqrt{2} & 1 \end{pmatrix}, \quad \Sigma_{3b} = \begin{pmatrix} 1 & 0 & -1/\sqrt{2} \\ 0 & 1 & -\Sigma_{jk}/\sqrt{2} \\ -1/\sqrt{2} & -\Sigma_{jk}/\sqrt{2} & 1 \end{pmatrix}.$$

**Theorem 3.** *Let  $X_j$  be truncated and  $X_k$  be continuous. Then  $\mathbb{E}(\hat{\tau}_{jk}) = F(\Sigma_{jk}; \Delta_j)$ , where*

$$F(\Sigma_{jk}; \Delta_j) = -2\Phi_2(-\Delta_j, 0; 1/\sqrt{2}) + 4\Phi_3(-\Delta_j, 0, 0; \Sigma_3),$$

$$\Delta_j = f_j(C_j) \text{ and}$$

$$\Sigma_3 = \begin{pmatrix} 1 & 1/\sqrt{2} & \Sigma_{jk}/\sqrt{2} \\ 1/\sqrt{2} & 1 & \Sigma_{jk} \\ \Sigma_{jk}/\sqrt{2} & \Sigma_{jk} & 1 \end{pmatrix}.$$

**Theorem 4.** *Let both  $X_j$  and  $X_k$  be truncated. Then  $\mathbb{E}(\hat{\tau}_{jk}) = F(\Sigma_{jk}; \Delta_j, \Delta_k)$ , where*

$$F(\Sigma_{jk}; \Delta_j, \Delta_k) = -2\Phi_4(-\Delta_j, -\Delta_k, 0, 0; \Sigma_{4a}) + 2\Phi_4(-\Delta_j, -\Delta_k, 0, 0; \Sigma_{4b}),$$

$$\Delta_j = f_j(C_j), \Delta_k = f_k(C_k) \text{ and}$$

$$\Sigma_{4a} = \begin{pmatrix} 1 & 0 & 1/\sqrt{2} & -\Sigma_{jk}/\sqrt{2} \\ 0 & 1 & -\Sigma_{jk}/\sqrt{2} & 1/\sqrt{2} \\ 1/\sqrt{2} & -\Sigma_{jk}/\sqrt{2} & 1 & -\Sigma_{jk} \\ -\Sigma_{jk}/\sqrt{2} & 1/\sqrt{2} & -\Sigma_{jk} & 1 \end{pmatrix}$$

and

$$\Sigma_{4b} = \begin{pmatrix} 1 & \Sigma_{jk} & 1/\sqrt{2} & \Sigma_{jk}/\sqrt{2} \\ \Sigma_{jk} & 1 & \Sigma_{jk}/\sqrt{2} & 1/\sqrt{2} \\ 1/\sqrt{2} & \Sigma_{jk}/\sqrt{2} & 1 & \Sigma_{jk} \\ \Sigma_{jk}/\sqrt{2} & 1/\sqrt{2} & \Sigma_{jk} & 1 \end{pmatrix}.$$

We also show that the inverse bridge function exists for all of the cases.

**Theorem 5.** *For any constants  $\Delta_j$  and  $\Delta_k$ , the bridge functions  $F(\Sigma_{jk})$  in Theorems 2–4 are strictly increasing in  $\Sigma_{jk} \in (-1, 1)$ , and therefore, the corresponding inverse functions  $F^{-1}(\Sigma_{jk})$  exist.*

Theorems 2–5 complement the results of Fan et al. (2017) summarized in Theorem 1 by adding three more cases (continuous/truncated, binary/truncated and truncated/truncated), thus allowing us to construct a rank-based estimator  $\hat{R}$  for  $\Sigma$  in the presence of mixed (continuous/binary/truncated) variables.

**Remark 2.** *Since  $\hat{R}$  is not guaranteed to be positive semidefinite, Fan et al. (2017) regularize  $\hat{R}$  by projecting it onto the cone of positive semidefinite matrices. We follow this approach using the `nearPD` function in the `Matrix` R package leading to estimator  $\hat{R}_p$ . Furthermore, we consider*

$$\tilde{R} = (1 - \rho)\hat{R}_p + \rho I \quad (3)$$

with a small value of  $\rho > 0$ , so that  $\tilde{R}$  is strictly positive definite. Throughout, we fix  $\rho = 0.01$ .

**Remark 3.** *As in the binary case,  $\Delta_j = f_j(C_j)$  is unknown for truncated variables. Similar to Fan et al. (2017), we use a plug-in estimator  $\hat{\Delta}_j$  based on the moment equation  $\mathbb{E}\{I(X_{ij} > 0)\} = \mathbb{P}(X_j > 0) = \mathbb{P}\{f_j(U_j) > \Delta_j\} = 1 - \Phi(\Delta_j)$ . Let  $n_{\text{nonzero}} = \sum_{i=1}^n I(X_{ij} > 0)$  for  $i = 1, \dots, n$ . Then we use  $\hat{\Delta}_j = \Phi^{-1}(1 - n_{\text{nonzero}}/n)$ .*

### 3.2 Semiparametric sparse canonical correlation analysis

Our proposal is based on formulating sparse canonical correlation analysis using latent correlation matrix from the Gaussian copula model for mixed data. On a population level, let  $\Sigma$  be the latent correlation matrix for  $(\mathbf{X}_1, \mathbf{X}_2) \sim \text{LNPN}(0, \Sigma, f, \mathbf{C})$  where each  $\mathbf{X}_1$  and  $\mathbf{X}_2$  follows one of the three data types: continuous, binary or truncated. In Section 3.1 we derived a rank-based estimator for  $\Sigma$ , which we propose to use within the sparse canonical correlation analysis framework (2).

Given the semiparametric estimator  $\tilde{R}$  in (3), we propose to find canonical vectors by solving

$$\underset{w_1, w_2}{\text{minimize}} \left\{ -w_1^\top \tilde{R}_{12} w_2 + \lambda_1 \|w_1\|_1 + \lambda_2 \|w_2\|_1 \right\} \quad \text{subject to} \quad w_1^\top \tilde{R}_1 w_1 \leq 1, \quad w_2^\top \tilde{R}_2 w_2 \leq 1. \quad (4)$$

While we focus only on the estimation of the first canonical pair, the subsequent canonical pairs can be found sequentially by using a deflation scheme as follows. Let  $\tilde{R}_{12}^{(1)} = \tilde{R}_{12}$  and let  $\hat{w}_1, \hat{w}_2$  be the  $(k-1)$ th estimated canonical pair. To estimate the  $k$ th pair for  $k > 1$ , form

$$\tilde{R}_{12}^{(k)} = \tilde{R}_{12}^{(k-1)} - (\hat{w}_1^\top \tilde{R}_{12}^{(k-1)} \hat{w}_2) \tilde{R}_1 \hat{w}_1 \hat{w}_2^\top \tilde{R}_2,$$

and solve (4) using  $\tilde{R}_{12}^{(k)}$  instead of  $\tilde{R}_{12}$ .

While problem (4) is not jointly convex in  $w_1$  and  $w_2$ , it is biconvex. Therefore, we propose to iteratively optimize over  $w_1$  and  $w_2$ . First, consider optimizing over  $w_1$  with  $w_2$  fixed.

**Proposition 1.** For a fixed  $w_2 \in \mathbb{R}^{p_2}$ , let

$$\hat{w}_1 = \underset{w_1}{\operatorname{argmin}} \left\{ -w_1^\top \tilde{R}_{12} w_2 + \lambda_1 \|w_1\|_1 \right\} \quad \text{subject to} \quad w_1^\top \tilde{R}_1 w_1 \leq 1. \quad (5)$$

This problem is equivalent to finding

$$\tilde{w}_1 = \underset{w_1}{\operatorname{argmin}} \left\{ (1/2) w_1^\top \tilde{R}_1 w_1 - w_1^\top \tilde{R}_{12} w_2 + \lambda_1 \|w_1\|_1 \right\}, \quad (6)$$

and then setting  $\hat{w}_1 = 0$  if  $\tilde{w}_1 = 0$ , and  $\hat{w}_1 = \tilde{w}_1 / (\tilde{w}_1^\top \tilde{R}_1 \tilde{w}_1)^{1/2}$  if  $\tilde{w}_1 \neq 0$ .

Both problems (5) and (6) are convex, but unlike (5), problem (6) is unconstrained. Furthermore, problem (6) is of the same form as the well-studied penalized LASSO problem (Tibshirani, 1996), which can be solved efficiently using for example the coordinate-descent algorithm. Hence, the proposed optimization algorithm for (4) can be viewed as a sequence of LASSO problems with rescaling. Given the value of  $w_2$  at iteration  $t$ , the updates at iteration  $t + 1$  have the form

$$\begin{aligned} \tilde{w}_1 &= \underset{w_1}{\operatorname{argmin}} \left\{ (1/2) w_1^\top \tilde{R}_1 w_1 - w_1^\top \tilde{R}_{12} w_2^{(t)} + \lambda_1 \|w_1\|_1 \right\}; \\ \hat{w}_1^{(t+1)} &= \tilde{w}_1 / (\tilde{w}_1^\top \tilde{R}_1 \tilde{w}_1)^{1/2}; \\ \tilde{w}_2 &= \underset{w_2}{\operatorname{argmin}} \left\{ (1/2) w_2^\top \tilde{R}_2 w_2 - w_2^\top \tilde{R}_{12}^\top \hat{w}_1^{(t+1)} + \lambda_2 \|w_2\|_1 \right\}; \\ \hat{w}_2^{(t+1)} &= \tilde{w}_2 / (\tilde{w}_2^\top \tilde{R}_2 \tilde{w}_2)^{1/2}. \end{aligned}$$

If a zero solution is obtained at any of the steps, the optimization algorithm stops, and both  $w_1$  and  $w_2$  are returned as zeroes. Otherwise, the algorithm proceeds until convergence, which is guaranteed due to biconvexity of (4) (Gorski et al., 2007).

We further describe a coordinate-descent algorithm for (6). Consider the KKT conditions (Boyd and Vandenberghe, 2004)

$$\tilde{R}_1 w_1 - \tilde{R}_{12} w_2 + \lambda_1 s_1 = 0,$$

where  $s_1$  is the subgradient of  $\|w_1\|_1$ . If  $\lambda_1 \geq \|\tilde{R}_{12} w_2\|_\infty$ , it follows that  $\tilde{w}_1 = 0$ . Otherwise, the  $i$ th element of  $w_1$  can be expressed through the other coordinates as

$$w_{1i} = S_{\lambda_1} \left\{ (\tilde{R}_{12})_i w_2^{(t)} - (\tilde{R}_1)_{i,-i} (w_1)_{-i} \right\},$$

where  $S_\lambda(t) = \operatorname{sign}(t) (|t| - \lambda)_+$  is the soft-thresholding operator,  $(R_{12})_i$  denotes the  $i$ th row of matrix  $R_{12}$  and  $(R_1)_{i,-i}$  denotes  $i$ th row of matrix  $R_1$  without the  $i$ th component that is  $(R)_{i,-i} = (R_{i1}, \dots, R_{i,i-1}, R_{i,i+1}, \dots, R_{ip})$ . The coordinate-descent algorithm proceeds by using the above formula to update one coordinate at a time until the convergence to a global optimum is achieved. This convergence is guaranteed due to convexity of the objective function and separability of the penalty with respect to coordinates (Tseng, 1988).



### 3.3 Selection of tuning parameters

Cross-validation is a popular approach to select the tuning parameter in LASSO. In our context, however, it amounts to performing a grid search over both  $\lambda_1$  and  $\lambda_2$ . Moreover, splitting the data as in cross-validation leads to too small a number of testing samples to construct the rank-based estimator of the latent correlation matrix. Instead, motivated by [Wilms and Croux \(2015\)](#), we propose to adapt the Bayesian information criterion to the canonical correlation analysis to avoid splitting the data and decrease computational costs.

For the Gaussian linear regression model, the Bayesian information criterion (BIC) has the form

$$\text{BIC} = -2\ell + \text{df} \log n,$$

where  $\text{df}$  indicate the number of parameters in the model, and  $\ell$  is the log-likelihood

$$\ell = \log L = -(n/2) \log \sigma^2 - \sum_{i=1}^n (y_i - X_i \beta)^2 / (2\sigma^2).$$

Two cases can be considered depending on whether the variance  $\sigma^2$  is known or unknown.

1. If  $\sigma^2$  is known, and the data are scaled so that  $\sigma^2 = 1$ , then

$$\text{BIC} = n^{-1} \sum_{i=1}^n (y_i - X_i \hat{\beta})^2 + \text{df} \log n/n.$$

2. If  $\sigma^2$  is unknown, using  $\hat{\sigma}_{\text{MLE}}^2 = n^{-1} \sum_{i=1}^n (y_i - X_i \beta)^2$  leads to

$$\text{BIC} = n \log \left\{ n^{-1} \sum_{i=1}^n (y_i - X_i \hat{\beta})^2 \right\} + \text{df} \log n.$$

[Wilms and Croux \(2015\)](#) use criterion 2 for canonical correlation analysis by substituting  $\|X_1 \hat{w}_1 - X_2 w_2\|_2^2/n$  instead of  $\sum_{i=1}^n (y_i - X_i \hat{\beta})^2/n$  for centered  $X_1$  and  $X_2$ . Since  $\|X_1 \hat{w}_1 - X_2 w_2\|_2^2/n = w_1^\top S_1 w_1 - 2w_1^\top S_{12} w_2 + w_2^\top S_2 w_2$ , and we use  $\tilde{R}$  instead of sample covariance matrix  $S$ , we substitute

$$f(\hat{w}_1) = \hat{w}_1^\top \tilde{R}_1 \hat{w}_1 - 2\hat{w}_1^\top \tilde{R}_{12} w_2 + w_2^\top \tilde{R}_2 w_2$$

instead of residual sum of squares. Furthermore, motivated by the performance of the adjusted degrees of freedom variance estimator in [Reid et al. \(2016\)](#), we also adjust  $f(\hat{w}_1)$  for the 2nd criterion leading to

$$\begin{aligned} \text{BIC1} &= f(\hat{w}_1) + \text{df}_{\hat{w}_1} \log n/n; \\ \text{BIC2} &= \log \left\{ \frac{n}{n - \text{df}_{\hat{w}_1}} f(\hat{w}_1) \right\} + \text{df}_{\hat{w}_1} \log n/n. \end{aligned}$$

Here  $\text{df}_{\hat{w}_1}$  coincide with the size of the support of  $\hat{w}_1$  ([Tibshirani and Taylor, 2012](#)). The BIC criteria for  $w_2$  are defined analogously to  $w_1$ .

We use both criteria in evaluating our approach. Given the selected criterion (either BIC1 or BIC2), we apply it sequentially at each step of the biconvex optimization algorithm of [Section 3.2](#), and each time select the tuning parameter corresponding to the smallest value of criterion.



## 4 Simulation studies

In this section we evaluate the performance of the following methods: (i) Classical canonical correlation analysis based on the sample covariance matrix; (ii) Canonical ridge available in the R package CCA (González et al., 2008); (iii) Sparse canonical correlation analysis of Witten et al. (2009) available in the R package PMA; (iv) Sparse canonical correlation analysis via Kendall’s  $\tau$  proposed in this paper. For our method, we evaluate both types of BIC criteria as described in Section 3.3.

We generate  $n = 100$  independent pairs  $(\mathbf{Z}_1, \mathbf{Z}_2) \in \mathbb{R}^{p_1+p_2}$  following

$$\begin{pmatrix} \mathbf{Z}_1 \\ \mathbf{Z}_2 \end{pmatrix} \sim N \left\{ \begin{pmatrix} 0 \\ 0 \end{pmatrix}, \begin{pmatrix} \Sigma_1 & \rho \Sigma_1 w_1 w_2^\top \Sigma_2 \\ \rho \Sigma_2 w_2 w_1^\top \Sigma_1 & \Sigma_2 \end{pmatrix} \right\}.$$

We consider two settings for the number of variables: low-dimensional ( $p_1 = p_2 = 25$ ) and high-dimensional ( $p_1 = p_2 = 100$ ). Each canonical vector  $w_g$  ( $g = 1, 2$ ) is defined by taking a vector of ones at the coordinates (1, 6, 11, 16, 21) and zeros elsewhere, and normalizing it such that  $w_g^\top \Sigma_g w_g = 1$ ; a similar model is used in Chen et al. (2013). We use an autoregressive structure for  $\Sigma_1 = \{\gamma^{|j-k|}\}_{j,k=1}^{p_1}$  and a block-diagonal structure for  $\Sigma_2 = \text{block-diag}(\Sigma_\gamma, \dots, \Sigma_\gamma)$ , where  $\Sigma_\gamma \in \mathbb{R}^{d \times d}$  is an equicorrelated matrix with value 1 on the diagonal and  $\gamma$  off the diagonal. We use five blocks of size  $d \in \{3, 3, 6, 6, 7\}$  for low-dimensional, and  $d \in \{12, 14, 21, 25, 28\}$  for high-dimensional setting. We set  $\gamma = 0.7$  for both  $\Sigma_1$  and  $\Sigma_2$ , similar results are obtained when autoregressive structure is substituted with identity matrix. We further randomly permute the order of variables in each  $Z_g$  to remove the covariance-induced ordering. The value of the canonical correlation is set at  $\rho = 0.9$ .

We consider transformations  $\mathbf{U}_g = f_g(\mathbf{Z}_g + c)$  with  $c$  being 0 or 1 with equal probability. The choice of  $c$  allows us to vary the proportion of zero values in truncated and binary variables from 5–80%. We consider three choices for  $f_g$ : (copula 0) no transformation,  $f_g(z) = z$  for  $g = 1, 2$ ; (copula 1) exponential transformation for  $\mathbf{U}_1$ ,  $f_1(z) = \exp(z)$ , and no transformation for  $\mathbf{U}_2$ ,  $f_2(z) = z$ ; (copula 2) exponential transformation for  $\mathbf{U}_1$ ,  $f_1(z) = \exp(z)$ , and cubic transformation for  $\mathbf{U}_2$ ,  $f_2(z) = z^3$ . Finally, we set  $\mathbf{X}_g$  to be equal to  $\mathbf{U}_g$  for continuous variable type, and dichotomize  $\mathbf{U}_g$  at value  $C$  to form binary/truncated  $\mathbf{X}_g$ . We set  $C = 0$  for copula 0 and 1, and  $C = 1.5$  for copula 2. For each case, we consider three combinations of variable types for  $\mathbf{X}_1/\mathbf{X}_2$ : truncated/truncated, truncated/continuous and truncated/binary.

To compare the methods performance, we evaluate expected out-of-sample correlation

$$\hat{\rho} = \frac{\hat{w}_1^\top \Sigma_{12} \hat{w}_2}{(\hat{w}_1^\top \Sigma_1 \hat{w}_1)^{1/2} (\hat{w}_2^\top \Sigma_2 \hat{w}_2)^{1/2}}, \quad (7)$$

and predictive loss

$$L(w_g, \hat{w}_g) = 1 - \frac{|\hat{w}_g^\top \Sigma_g w_g|}{(\hat{w}_g^\top \Sigma_g \hat{w}_g)^{1/2}} \quad (g = 1, 2); \quad (8)$$

similar loss function is used in Gao et al. (2017). Since  $w_g^\top \Sigma_g w_g = 1$ ,  $L(w_g, \hat{w}_g) \in [0, 1]$  with  $L(w_g, \hat{w}_g) = 0$  if  $\hat{w}_g = w_g$ . We also evaluate the variable selection performance using the selected model size, true-positive rate and true-negative rate defined as

$$\text{TPR}_g = \frac{\#\{j : \hat{w}_{gj} \neq 0 \text{ and } w_{gj} \neq 0\}}{\#\{j : w_{gj} \neq 0\}}, \quad \text{TNR}_g = \frac{\#\{j : \hat{w}_{gj} = 0 \text{ and } w_{gj} = 0\}}{\#\{j : w_{gj} = 0\}} \quad (g = 1, 2).$$

The results for the truncated/truncated case over 100 replications are presented in Figures 1–3: the results for the other cases and deferred to Appendix B.

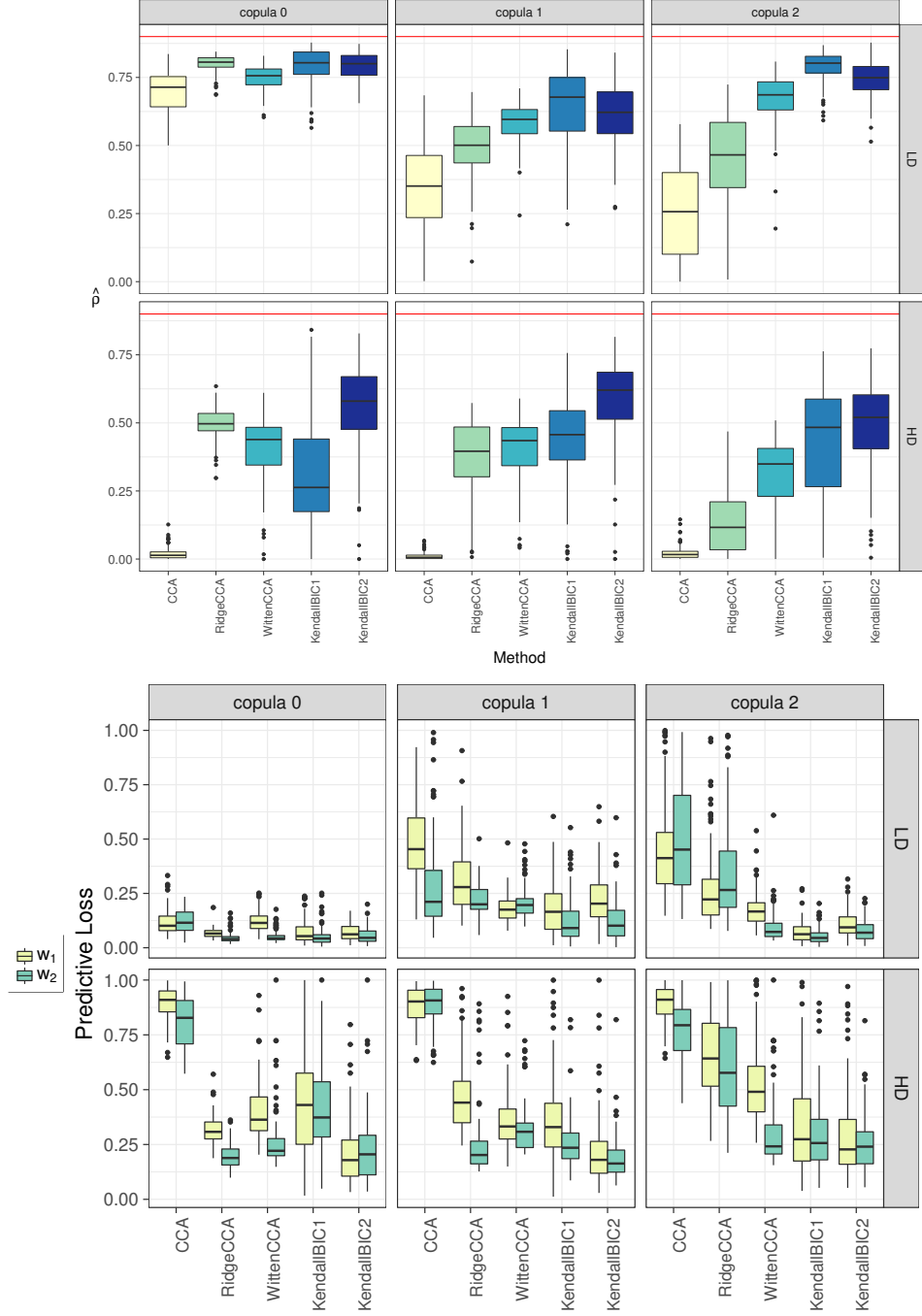


Figure 1: Truncated/truncated case. **Top:** The value of  $\hat{\rho}$  from (7). The horizontal lines indicate the true canonical correlation value  $\rho = 0.9$ . **Bottom:** The value of predictive loss (8). Results over 100 replications. CCA: Sample canonical correlation analysis; RidgeCCA: Canonical ridge of González et al. (2008); WittenCCA: method of Witten et al. (2009); KendallBIC1, KendallBIC2: proposed method with tuning parameter selected using either BIC1 or BIC2 criterion; LD: low-dimensional setting ( $p_1 = p_2 = 25$ ); HD: high-dimensional setting ( $p_1 = p_2 = 100$ ).

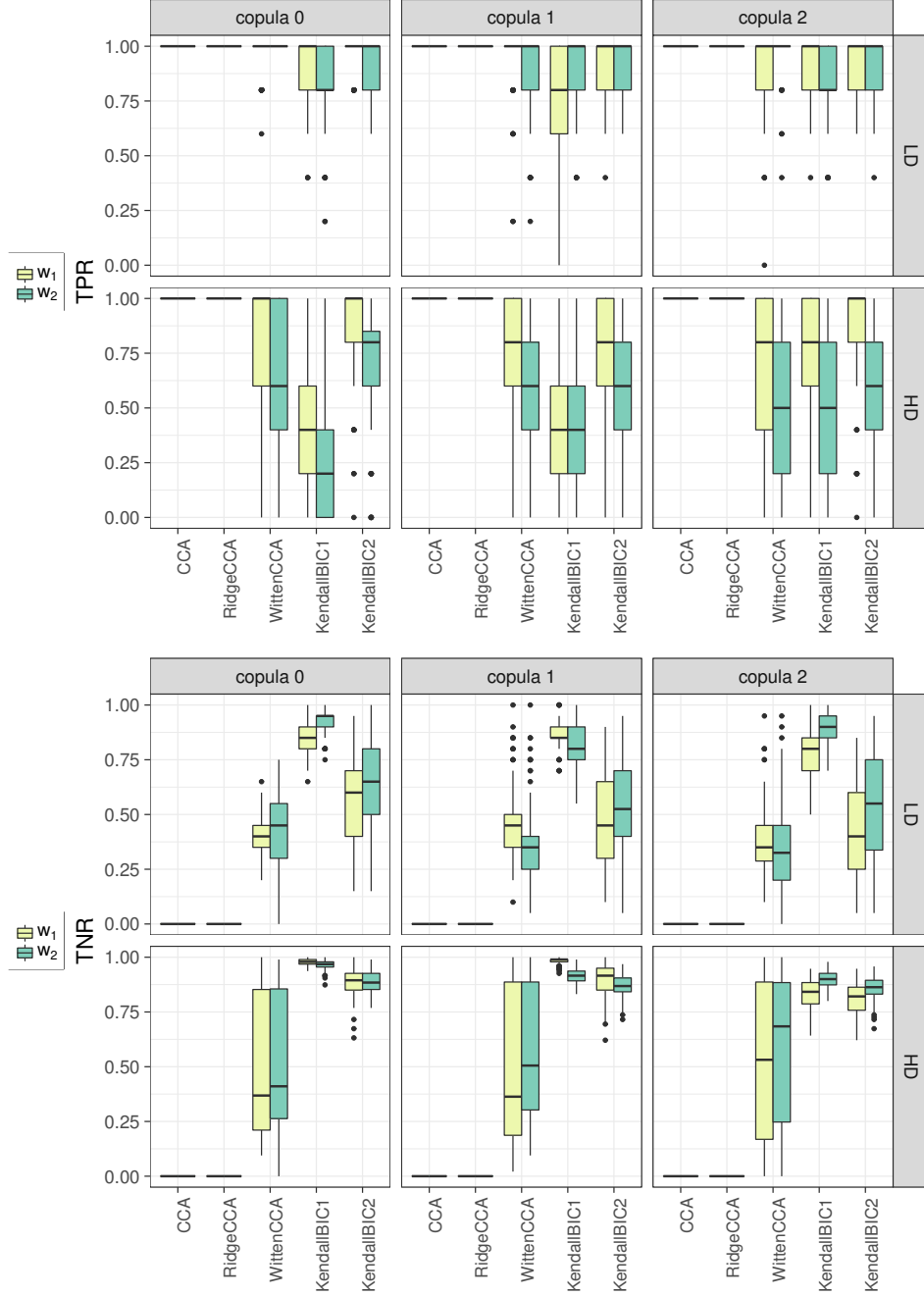


Figure 2: Truncated/truncated case. **Top:** True positive rate (TPR); **Bottom:** True negative rate (TNR). Results over 100 replications. CCA: Sample canonical correlation analysis; RidgeCCA: Canonical Ridge of [González et al. \(2008\)](#); WittenCCA: method of [Witten et al. \(2009\)](#); Kendall-BIC1, KendallBIC2: proposed method with tuning parameter selected using either BIC1 or BIC2 criterion; LD: low-dimensional setting ( $p_1 = p_2 = 25$ ); HD: high-dimensional setting ( $p_1 = p_2 = 100$ ).

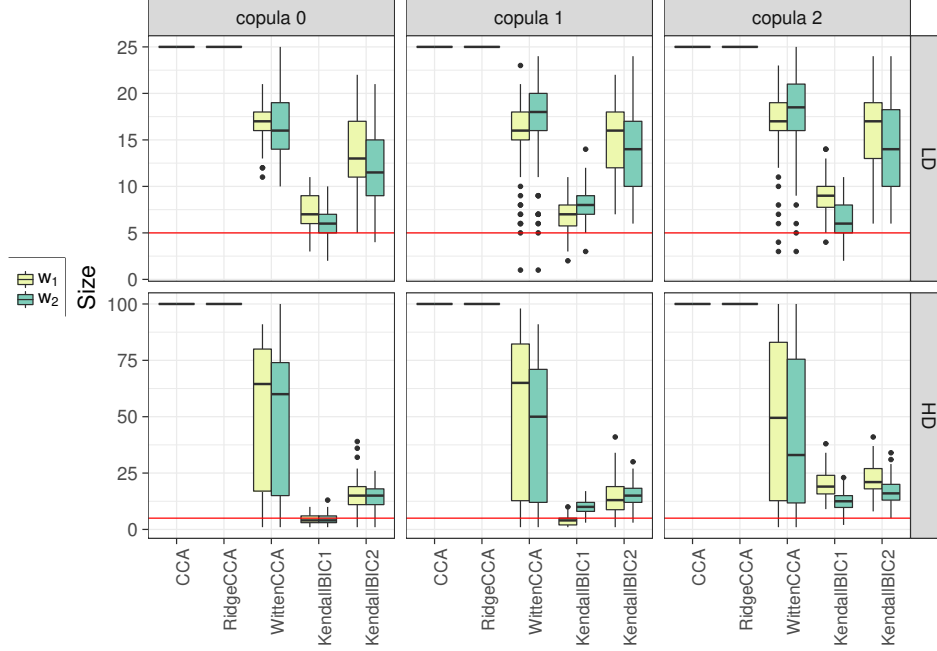


Figure 3: Truncated/truncated case. Selected model size over 100 replications. The horizontal lines indicate the true model size 5. CCA: Sample canonical correlation analysis; RidgeCCA: Canonical Ridge of [González et al. \(2008\)](#); WittenCCA: method of [Witten et al. \(2009\)](#); KendallBIC1, KendallBIC2: proposed method with tuning parameter selected using either BIC1 or BIC2 criterion; LD: low-dimensional setting ( $p_1 = p_2 = 25$ ); HD: high-dimensional setting ( $p_1 = p_2 = 100$ ).

From Figure 1, all methods perform better in the absence of data transformation (copula 0) compared to cases where transformation is applied (copula 1 and 2). Similarly, the performance deteriorates with increased dimensions leading to smaller values of  $\hat{\rho}$ , larger predictive losses and worse true positive rates. The classical canonical correlation analysis performs especially poorly in high-dimensional settings with  $\hat{\rho}$  being very close to 0 and predictive loss being close to 1 for both  $w_1$  and  $w_2$ . Canonical ridge works well in the copula 0 setting, however its performance is strongly affected in the presence of transformations (copula 1 and 2). Witten’s method outperforms canonical ridge in the presence of transformations, however works worse than both variants of our approach. Overall, our method with BIC1 attains the highest values of  $\hat{\rho}$  in low-dimensional settings, whereas BIC2 is the highest in high-dimensional settings. Unlike the classical canonical correlation and canonical ridge, both Witten’s and our method perform variable selection. Unexpected to us, the number of selected variables varies significantly across replications for Witten’s method (Figure 3), leading to significant variations in true positive and true negative rates. In all cases BIC1 leads to the sparsest model and the highest true negative rate. On the other hand, since BIC1 sometimes misses true variables, especially in the high-dimensional settings, BIC2 shows more accurate values of  $\hat{\rho}$  and smaller predictive loss, see Figure 1. In summary, BIC1 works better for variable selection, whereas BIC2 works better for prediction.

Table 1: Mean support sizes and values of  $\hat{\rho}_{\text{test}}$ 's over 100 random splits of breast cancer data, standard deviation is given in parentheses

Method	Selected Genes	Selected micro RNAs	$\hat{\rho}_{\text{test}}$
CCA	891 (0.00)	431 (0.00)	0.0219 (0.111)
RidgeCCA	891 (0.00)	431 (0.00)	0.704 (0.129)
WittenCCA	368.91 (195.38)	179.86 (100.95)	0.787 (0.0448)
KendallBIC1	83.73 (23.43)	6.11 (1.95)	0.888 (0.0438)
KendallBIC2	106.03 (10.86)	105.90 (10.20)	0.926 (0.231)

## 5 Application to TCGA data

The Cancer Genome Atlas (TCGA) project collects data from multiple platforms using high-throughput sequencing technologies. We consider gene expression data ( $p_1 = 891$ ) and micro RNA data ( $p_2 = 431$ ) for  $n = 500$  matched subjects from TCGA breast cancer database. We treat gene expression data as continuous and micro RNA data as truncated continuous. The range of proportions of zero values contained in each variable in micro RNA data is 0 – 49.8%. The subjects belong to one of the 5 breast cancer subtypes: Normal, Basal, Her2, LumA and LumB, with 37 subjects having missing subtype information (denoted as NA). The goal of the analysis is to characterize the association between gene expression and micro RNA data, and investigate whether this association is related to breast cancer subtypes.

To investigate the performance of our method relative to other approaches, we randomly split the data 100 times. Each time 400 samples are used for training, and the remaining 100 test samples are used to assess the found association via

$$\hat{\rho}_{\text{test}} = \frac{\hat{w}_{1,\text{train}}^\top \Sigma_{12,\text{test}} \hat{w}_{2,\text{train}}}{(\hat{w}_{1,\text{train}}^\top \Sigma_{1,\text{test}} \hat{w}_{1,\text{train}})^{1/2} (\hat{w}_{2,\text{train}}^\top \Sigma_{2,\text{test}} \hat{w}_{2,\text{train}})^{1/2}}.$$

Here  $\Sigma_{\text{test}}$  is evaluated based on the test samples, and is either the rank-based estimator  $\tilde{R}$  for our method, or the sample covariance matrix for other methods. We also compare the number of selected genes and micro RNAs, and the results are presented in Table 1.

As expected, neither the sample canonical correlation analysis nor the canonical ridge method perform variable selection. In addition,  $\hat{\rho}_{\text{test}}$  is very close to 0 for sample canonical correlation, confirming poor performance of the method. Canonical ridge leads to significantly higher values of  $\hat{\rho}_{\text{test}}$  demonstrating the advantage of added regularization, however it still has smaller correlation values compared to other approaches. The method of Witten et al. (2009) leads to higher correlation values compared to both sample canonical correlation analysis and canonical ridge, however it still selects a significant number of variables, with highly variable model sizes across replications. We suspect this is due to the use of permutation-based algorithm for tuning parameter selection: similar behaviour is observed in Section 4. Finally, the values of  $\hat{\rho}_{\text{test}}$  are the highest for both variations of our method, confirming that found association is not due to over-fitting as it generalizes

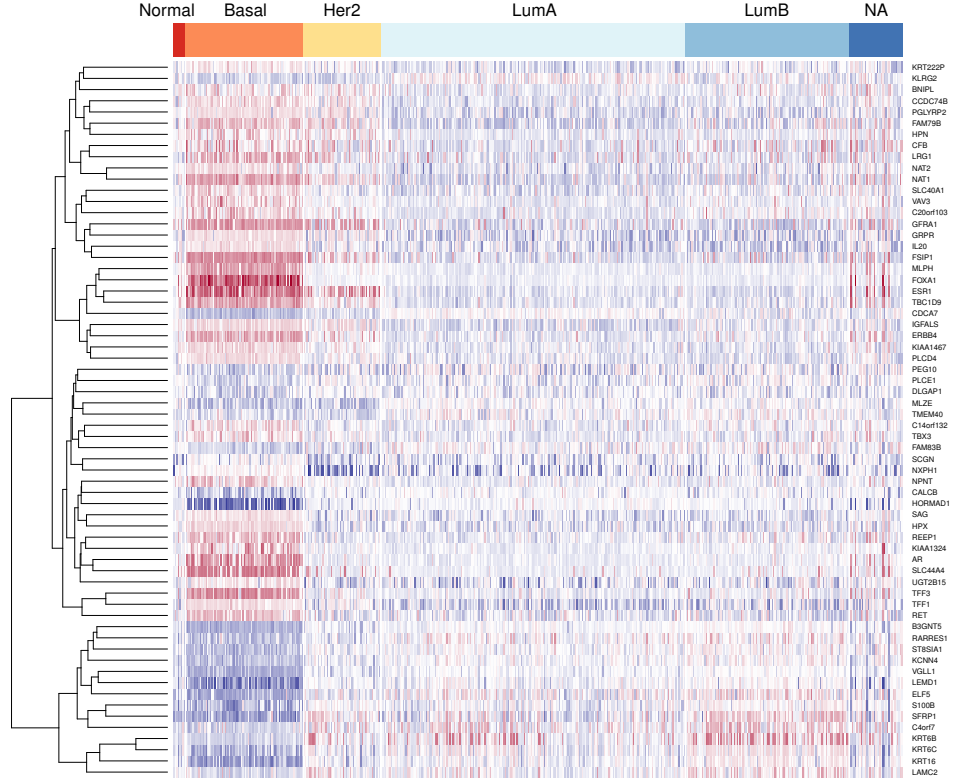


Figure 4: A heatmap of 64 genes selected by the proposed approach when using the BIC1 criterion. Dissimilarity measure is set as  $1 - \tau^2$  with  $\tau$  being the Kendall's  $\tau$ , and the Ward linkage is used.

well to out-of-sample data. At the same time, both BIC criteria in our method result in sparsest models with smallest variability in model size across replications. While BIC2 criterion leads to the largest out-of-sample correlation value, the BIC1 criterion leads to the sparsest model. In light of these results and results of Section 4, we conclude that BIC1 works well for variable selection, whereas BIC2 works well for prediction.

We further apply our method with the BIC1 criterion using the full set of  $n = 500$  samples, leading to the selection of 64 genes and 8 micro RNAs. Figures 4 and 5 show heatmaps of selected variables for each platform, with samples ordered by their respective cancer subtype. The heatmaps show clear separation between Basal and other subtypes, suggesting that found association is relevant to cancer biology.

Some of the selected genes and micro RNAs can be found in recent literature which supports their association with breast cancer. For example, [Xiao et al. \(2018\)](#) identify hsa-miR-452-5p in the analysis of estrogen receptor subtypes of breast cancer, and [Manvati et al. \(2015\)](#) demonstrate negative correlation of hsa-miR-24-2 with both metastasis and increasing nodes in sporadic breast tumours. As for hsa-miR-135b, not only it is reported to be related to breast cancer cell growth

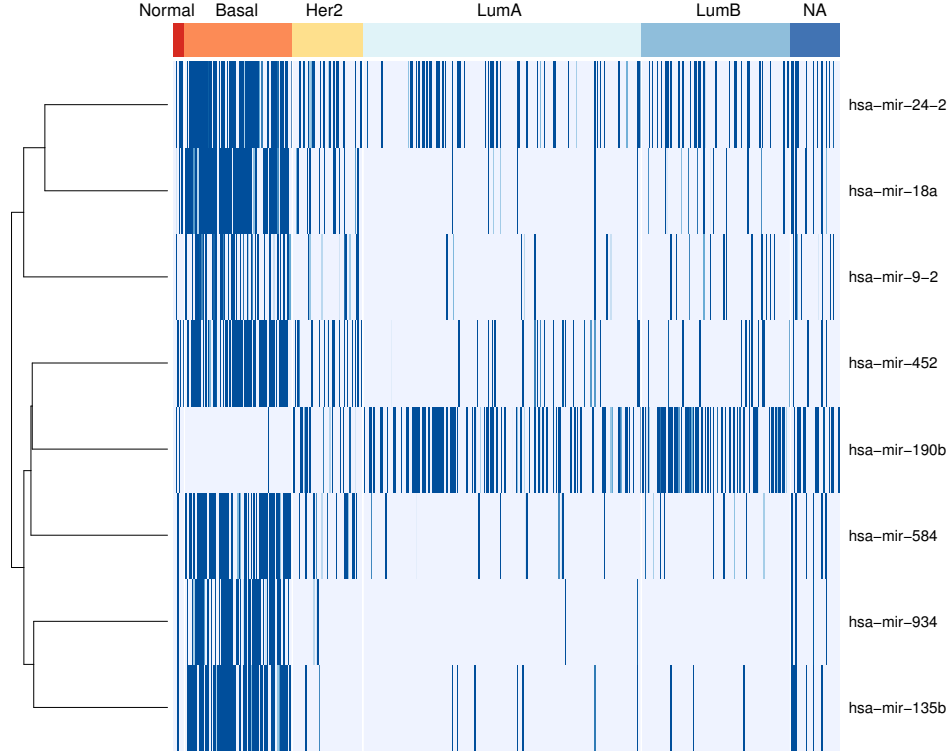


Figure 5: A heatmap of 8 micro RNAs selected by the proposed approach when using theBIC1 criterion. Dissimilarity measure is set as  $1 - \tau^2$  with  $\tau$  being the Kendall's  $\tau$ , and the Ward linkage is used. Colors are assigned based on variable-specific quantiles.

(Aakula et al., 2015; Hua et al., 2016), but it is also demonstrated to regulate estrogen receptor  $\alpha$  gene ESR1 (Aakula et al., 2015), which coincidentally is among the 64 genes selected by our approach. Some other genes among the selected ones that demonstrate association with breast cancer according to previous research are ERBB4, FOXA1, UGT2B15 and ELF5 (Hu et al., 2016; Kim et al., 2016; Piggin et al., 2016).

## 6 Discussion

One of the main contributions of this work is the proposed truncated Gaussian copula model for the zero-inflated data, and corresponding development of a rank-based estimator for the latent correlation matrix. While our focus is on canonical correlation analysis, the derived estimator can be used in conjunction with other covariance-based approaches. For example it can be used for constructing graphical models as in Fan et al. (2017) in cases where some or all of the vari-



ables have an excess of zeroes. Micro RNA data is one example that we have explored in this work, however another prominent example is microbiome abundance data. It would be of interest to further explore the potential of our modeling approach in different application areas. The R package `mixedCCA` with method's implementation is available from the authors github page <https://github.com/irinagain/mixedCCA>.

## Acknowledgements

Yoon's research was funded by a grant from the National Cancer Institute (T32-CA090301). Carroll's research was supported by a grant from the National Cancer Institute (U01-CA057030). Carroll is also Distinguished Professor, School of Mathematical and Physical Sciences, University of Technology Sydney, Broadway NSW 2007, Australia. Gaynanova's research was supported by National Science Foundation grant DMS-1712943.

## Appendix A Technical details

**Proof of Theorem 2.** Without loss of generality, let  $j = 1$  and  $k = 2$ . By the definition of Kendall's  $\tau$ ,

$$\tau_{12} = \mathbb{E}(\hat{\tau}_{12}) = \mathbb{E} \left[ 2\{n(n-1)\}^{1/2} \sum_{1 \leq i < i' \leq n} \text{sign} \{ (X_{i1} - X'_{i1})(X_{i2} - X'_{i2}) \} \right].$$

Since  $X_2$  is binary,

$$\begin{aligned} \text{sign}(X_2 - X'_2) &= I(U_2 > C_2, U'_2 \leq C_2) - I(U_2 \leq C_2, U'_2 > C_2) \\ &= I(U_2 > C_2) - I(U_2 > C_2, U'_2 > C_2) - I(U'_2 > C_2) + I(U_2 > C_2, U'_2 > C_2) \\ &= I(U_2 > C_2) - I(U'_2 > C_2), \end{aligned}$$

thus

$$\tau_{12} = \mathbb{E} [\text{sign}(X_1 - X'_1) I(U_2 > C_2)] - \mathbb{E} [\text{sign}(X_1 - X'_1) I(U'_2 > C_2)]. \quad (9)$$

Since  $X_1$  is truncated,  $C_1 > 0$  and

$$\begin{aligned} \text{sign}(X_1 - X'_1) &= -I(X_1 = 0, X'_1 > 0) + I(X_1 > 0, X'_1 = 0) + I(X_1 > 0, X'_1 > 0) \text{sign}(X_1 - X'_1) \\ &= -I(X_1 = 0) + I(X'_1 = 0) + I(X_1 > 0, X'_1 > 0) \text{sign}(X_1 - X'_1). \end{aligned} \quad (10)$$

Since we assume that  $\mathbf{U} = (U_1, \dots, U_p)^\top \sim \text{NPN}(0, \Sigma, f)$ , let  $Z = f(U)$  where  $Z \sim N(0, \Sigma)$  for the rest of the proofs. Since  $f$  is monotonically increasing,  $\text{sign}(X_1 - X'_1) = \text{sign}(Z_1 - Z'_1)$ . Combining (9) and (10) yields

$$\begin{aligned} \tau_{12} &= -2\mathbb{E} \{ I(X_1 = 0) I(U_2 > C_2) \} + 2\mathbb{E} \{ I(X'_1 = 0) I(U_2 > C_2) \} \\ &\quad + \mathbb{E} \{ I(X_1 > 0, X'_1 > 0) \text{sign}(Z_1 - Z'_1) I(U_2 > C_2) \} \\ &\quad - \mathbb{E} \{ I(X_1 > 0, X'_1 > 0) \text{sign}(Z_1 - Z'_1) I(U'_2 > C_2) \}. \end{aligned}$$

From the definition of  $U$ , let  $Z_j = f_j(U_j)$  and  $\Delta_j = f_j(C_j)$  for  $j = 1, 2$ . Using  $\text{sign}(x) = 2I(x > 0) - 1$ , we obtain

$$\begin{aligned}\tau_{12} = & -2\mathbb{E}\{I(Z_1 \leq \Delta_1, Z_2 > \Delta_2)\} + 2\mathbb{E}\{I(Z'_1 \leq \Delta_1, Z_2 > \Delta_2)\} \\ & + 2\mathbb{E}\{I(Z_1 > \Delta_1, Z'_1 > \Delta_1, Z_1 - Z'_1 > 0)I(Z_2 > \Delta_2)\} \\ & - 2\mathbb{E}\{I(Z_1 > \Delta_1, Z'_1 > \Delta_1, Z_1 - Z'_1 > 0)I(Z'_2 > \Delta_2)\}.\end{aligned}$$

Since  $Z'_1 > \Delta_1, Z_1 - Z'_1 > 0$  implies  $Z_1 > \Delta_1$ , so  $\tau_{12}$  can be further simplified as

$$\begin{aligned}\tau_{12} = & -2\mathbb{E}\{I(Z_1 \leq \Delta_1, Z_2 > \Delta_2)\} + 2\mathbb{E}\{I(Z'_1 \leq \Delta_1, Z_2 > \Delta_2)\} \\ & + 2\mathbb{E}\{I(Z'_1 > \Delta_1, Z_2 > \Delta_2, Z_1 - Z'_1 > 0)\} - 2\mathbb{E}\{I(Z'_1 > \Delta_1, Z'_2 > \Delta_2, Z_1 - Z'_1 > 0)\}.\end{aligned}$$

Since  $\{(Z'_1 - Z_1)/\sqrt{2}, -Z'_1\}$ ,  $\{(Z'_1 - Z_1)/\sqrt{2}, -Z_2\}$  and  $\{(Z'_1 - Z_1)/\sqrt{2}, -Z'_2\}$  are standard bivariate normally distributed with correlation  $-1/\sqrt{2}$ ,  $\Sigma_{12}/\sqrt{2}$  and  $-\Sigma_{12}/\sqrt{2}$  respectively, by the definition of  $\Phi(\cdot)$  and  $\Phi_2(\cdot, \cdot; r)$ , we have that

$$\begin{aligned}\tau_{12} = & 2\Phi_2(\Delta_1, -\Delta_2; -\Sigma_{12}) - 2\Phi(\Delta_1)\Phi(-\Delta_2) \\ & + 2\Phi_3\left\{-\Delta_1, -\Delta_2, 0; \begin{pmatrix} 1 & 0 & -1/\sqrt{2} \\ 0 & 1 & \Sigma_{12}/\sqrt{2} \\ -1/\sqrt{2} & \Sigma_{12}/\sqrt{2} & 1 \end{pmatrix}\right\} \\ & - 2\Phi_3\left\{-\Delta_1, -\Delta_2, 0; \begin{pmatrix} 1 & \Sigma_{12} & -1/\sqrt{2} \\ \Sigma_{12} & 1 & -\Sigma_{12}/\sqrt{2} \\ -1/\sqrt{2} & -\Sigma_{12}/\sqrt{2} & 1 \end{pmatrix}\right\}.\end{aligned}\tag{11}$$

Using that  $\Phi(\Delta_1) + \Phi(-\Delta_1) = 1$ ,  $\Phi(\Delta_1) = \Phi_2(\Delta_1, \Delta_2; \Sigma_{12}) + \Phi_2(\Delta_1, -\Delta_2; -\Sigma_{12})$  and

$$\begin{aligned}\Phi_2(\Delta_1, \Delta_2; \Sigma_{12}) = & \Phi_3\left\{\Delta_1, \Delta_2, \Delta_3; \begin{pmatrix} 1 & \Sigma_{12} & \Sigma_{13} \\ \Sigma_{12} & 1 & \Sigma_{23} \\ \Sigma_{13} & \Sigma_{23} & 1 \end{pmatrix}\right\} \\ & + \Phi_3\left\{\Delta_1, \Delta_2, -\Delta_3; \begin{pmatrix} 1 & \Sigma_{12} & -\Sigma_{13} \\ \Sigma_{12} & 1 & -\Sigma_{23} \\ -\Sigma_{13} & -\Sigma_{23} & 1 \end{pmatrix}\right\}\end{aligned}\tag{12}$$

we further simplify as

$$\begin{aligned}F(\Sigma_{12}; \Delta_1, \Delta_2) = & 2\{1 - \Phi(\Delta_1)\}\Phi(\Delta_2) \\ & - 2\Phi_3\left\{-\Delta_1, \Delta_2, 0; \begin{pmatrix} 1 & -\Sigma_{12} & 1/\sqrt{2} \\ -\Sigma_{12} & 1 & -\Sigma_{12}/\sqrt{2} \\ 1/\sqrt{2} & -\Sigma_{12}/\sqrt{2} & 1 \end{pmatrix}\right\} \\ & - 2\Phi_3\left\{-\Delta_1, \Delta_2, 0; \begin{pmatrix} 1 & 0 & -1/\sqrt{2} \\ 0 & 1 & -\Sigma_{12}/\sqrt{2} \\ -1/\sqrt{2} & -\Sigma_{12}/\sqrt{2} & 1 \end{pmatrix}\right\}.\end{aligned}$$

□

**Proof of Theorem 3.** Without loss of generality, we set  $j = 1$  and  $k = 2$ . Plugging (10) into the definition of the population Kendall's  $\tau_{12}$  and using  $\text{sign}(X_1 - X'_1) = \text{sign}(Z_1 - Z'_1)$ , we find

$$\begin{aligned}\tau_{12} &= -\mathbb{E} \{I(Z_1 \leq \Delta_1) \text{sign}(Z_2 - Z'_2)\} + \mathbb{E} \{I(Z'_1 \leq \Delta_1) \text{sign}(Z_2 - Z'_2)\} \\ &\quad + \mathbb{E} \{I(Z_1 > \Delta_1, Z'_1 > \Delta_1) \text{sign}(Z_1 - Z'_1) \text{sign}(Z_2 - Z'_2)\}.\end{aligned}$$

Using  $\text{sign}(x) = 2I(x > 0) - 1$ , it holds that

$$\begin{aligned}\tau_{12} &= -2\mathbb{E} \{I(Z_1 \leq \Delta_1, Z'_2 - Z_2 < 0)\} + 2\mathbb{E} \{I(Z'_1 \leq \Delta_1, Z'_2 - Z_2 < 0)\} \\ &\quad + \mathbb{E} \{I(Z_1 > \Delta_1, Z'_1 > \Delta_1) \text{sign}(Z_1 - Z'_1) \text{sign}(Z_2 - Z'_2)\}.\end{aligned}$$

It remains to show that the last term can be rewritten using cumulative normal distribution functions. The last term consists of four terms,

$$\begin{aligned}&\mathbb{E} \{I(Z_1 > \Delta_1, Z'_1 > \Delta_1) \text{sign}(Z_1 - Z'_1) \text{sign}(Z_2 - Z'_2)\} \\ &= \mathbb{P}(Z_1 > \Delta_1, Z'_1 > \Delta_1, Z_1 - Z'_1 > 0, Z_2 - Z'_2 > 0) \\ &\quad + \mathbb{P}(Z_1 > \Delta_1, Z'_1 > \Delta_1, Z_1 - Z'_1 < 0, Z_2 - Z'_2 < 0) \\ &\quad - \mathbb{P}(Z_1 > \Delta_1, Z'_1 > \Delta_1, Z_1 - Z'_1 > 0, Z_2 - Z'_2 < 0) \\ &\quad - \mathbb{P}(Z_1 > \Delta_1, Z'_1 > \Delta_1, Z_1 - Z'_1 < 0, Z_2 - Z'_2 > 0).\end{aligned}$$

Consider the first term

$$\begin{aligned}&\mathbb{P}(Z_1 > \Delta_1, Z'_1 > \Delta_1, Z_1 - Z'_1 > 0, Z_2 - Z'_2 > 0) \\ &= \mathbb{P}(Z'_1 > \Delta_1, Z_1 - Z'_1 > 0, Z_2 - Z'_2 > 0) - \mathbb{P}(Z_1 \leq \Delta_1, Z'_1 > \Delta_1, Z_1 - Z'_1 > 0, Z_2 - Z'_2 > 0) \\ &= \mathbb{P}(Z'_1 > \Delta_1, Z_1 - Z'_1 > 0, Z_2 - Z'_2 > 0).\end{aligned}$$

The last equality comes from fact that  $Z_1 - Z'_1 > 0$  cannot hold when  $Z_1 \leq \Delta_1$  and  $Z'_1 > \Delta_1$ , and this trick can be applied for all four terms leading to

$$\begin{aligned}&\mathbb{E} \{I(Z_1 > \Delta_1, Z'_1 > \Delta_1) \text{sign}(Z_1 - Z'_1) \text{sign}(Z_2 - Z'_2)\} \\ &= \mathbb{P}(-Z'_1 < \Delta_1, Z'_1 - Z_1 < 0, Z'_2 - Z_2 < 0) + \mathbb{P}(-Z_1 < \Delta_1, Z_1 - Z'_1 < 0, Z_2 - Z'_2 < 0) \\ &\quad - \mathbb{P}(-Z'_1 < \Delta_1, Z'_1 - Z_1 < 0, Z_2 - Z'_2 < 0) - \mathbb{P}(-Z_1 < \Delta_1, Z_1 - Z'_1 < 0, Z'_2 - Z_2 < 0).\end{aligned}$$

Using the definition of  $\Phi(\cdot)$  and  $\Phi_2(\cdot, \cdot; t)$ ,

$$\begin{aligned}\tau_{12} &= -2\Phi_2(\Delta_1, 0; -\Sigma_{12}/\sqrt{2}) + 2\Phi_2(\Delta_1, 0; \Sigma_{12}/\sqrt{2}) \\ &\quad + 2\Phi_3 \left\{ -\Delta_1, 0, 0; \begin{pmatrix} 1 & -1/\sqrt{2} & -\Sigma_{12}/\sqrt{2} \\ -1/\sqrt{2} & 1 & \Sigma_{12} \\ -\Sigma_{12}/\sqrt{2} & \Sigma_{12} & 1 \end{pmatrix} \right\} \\ &\quad - 2\Phi_3 \left\{ -\Delta_1, 0, 0; \begin{pmatrix} 1 & -1/\sqrt{2} & \Sigma_{12}/\sqrt{2} \\ -1/\sqrt{2} & 1 & -\Sigma_{12} \\ \Sigma_{12}/\sqrt{2} & -\Sigma_{12} & 1 \end{pmatrix} \right\}\end{aligned}$$

The second property in (12) yields

$$\begin{aligned}-2\Phi_2(\Delta_1, 0; -\Sigma_{12}/\sqrt{2}) &= -2\Phi(0) + 2\Phi_2(-\Delta_1, 0; \Sigma_{12}/\sqrt{2}) \\ 2\Phi_2(\Delta_1, 0; \Sigma_{12}/\sqrt{2}) &= 2\Phi(0) - 2\Phi_2(-\Delta_1, 0; -\Sigma_{12}/\sqrt{2}),\end{aligned}$$

and we can simplify further using the third property in (12).

$$\begin{aligned}
& 2\Phi_2(-\Delta_1, 0; \Sigma_{12}/\sqrt{2}) - 2\Phi_3 \left\{ -\Delta_1, 0, 0; \begin{pmatrix} 1 & -1/\sqrt{2} & \Sigma_{12}/\sqrt{2} \\ -1/\sqrt{2} & 1 & -\Sigma_{12} \\ \Sigma_{12}/\sqrt{2} & -\Sigma_{12} & 1 \end{pmatrix} \right\} \\
&= 2\Phi_3 \left\{ -\Delta_1, 0, 0; \begin{pmatrix} 1 & 1/\sqrt{2} & \Sigma_{12}/\sqrt{2} \\ 1/\sqrt{2} & 1 & \Sigma_{12} \\ \Sigma_{12}/\sqrt{2} & \Sigma_{12} & 1 \end{pmatrix} \right\} \\
&- 2\Phi_2(-\Delta_1, 0; -\Sigma_{12}/\sqrt{2}) + 2\Phi_3 \left\{ -\Delta_1, 0, 0; \begin{pmatrix} 1 & -1/\sqrt{2} & -\Sigma_{12}/\sqrt{2} \\ -1/\sqrt{2} & 1 & \Sigma_{12} \\ -\Sigma_{12}/\sqrt{2} & \Sigma_{12} & 1 \end{pmatrix} \right\} \\
&= -2\Phi_3 \left\{ -\Delta_1, 0, 0; \begin{pmatrix} 1 & 1/\sqrt{2} & -\Sigma_{12}/\sqrt{2} \\ 1/\sqrt{2} & 1 & -\Sigma_{12} \\ -\Sigma_{12}/\sqrt{2} & -\Sigma_{12} & 1 \end{pmatrix} \right\}.
\end{aligned}$$

Since

$$\begin{aligned}
& -2\Phi_3 \left\{ -\Delta_1, 0, 0; \begin{pmatrix} 1 & 1/\sqrt{2} & -\Sigma_{12}/\sqrt{2} \\ 1/\sqrt{2} & 1 & -\Sigma_{12} \\ -\Sigma_{12}/\sqrt{2} & -\Sigma_{12} & 1 \end{pmatrix} \right\} \\
&= -2\Phi_2(-\Delta_1, 0; 1/\sqrt{2}) + 2\Phi_3 \left\{ -\Delta_1, 0, 0; \begin{pmatrix} 1 & 1/\sqrt{2} & \Sigma_{12}/\sqrt{2} \\ 1/\sqrt{2} & 1 & \Sigma_{12} \\ \Sigma_{12}/\sqrt{2} & \Sigma_{12} & 1 \end{pmatrix} \right\},
\end{aligned}$$

we finally obtain

$$\tau_{12} = -2\Phi_2(-\Delta_1, 0; 1/\sqrt{2}) + 4\Phi_3 \left\{ -\Delta_1, 0, 0; \begin{pmatrix} 1 & 1/\sqrt{2} & \Sigma_{12}/\sqrt{2} \\ 1/\sqrt{2} & 1 & \Sigma_{12} \\ \Sigma_{12}/\sqrt{2} & \Sigma_{12} & 1 \end{pmatrix} \right\}.$$

□

**Proof of Theorem 4.** Without loss of generality, we set  $j = 1$  and  $k = 2$ . By the definition,

$$\tau_{12} = \mathbb{E}(\widehat{\tau}_{12}) = \mathbb{E} \left[ 2\{n(n-1)\}^{1/2} \sum_{1 \leq i < i' \leq n} \text{sign} \{ (X_{i1} - X'_{i1})(X_{i2} - X'_{i2}) \} \right].$$

Plugging (10) into the previous display and rearranging yields

$$\begin{aligned}
\tau_{12} &= \mathbb{E} \{ 2I(X_1 = 0, X_2 = 0) - 2I(X_1 = 0)I(X'_2 = 0) \} \\
&- \mathbb{E} \{ 2I(X_1 = 0, X_2 > 0, X'_2 > 0) \text{sign}(X_2 - X'_2) \} \\
&- \mathbb{E} \{ 2I(X_2 = 0, X_1 > 0, X'_1 > 0) \text{sign}(X_1 - X'_1) \} \\
&+ \mathbb{E} \{ I(X_1 > 0, X'_1 > 0, X_2 > 0, X'_2 > 0) \text{sign}(X_1 - X'_1) \text{sign}(X_2 - X'_2) \}.
\end{aligned}$$

It can be rewritten in terms of variable  $Z$  using the definition of variable  $X$ ,

$$\begin{aligned}
\tau_{12} &= \mathbb{E} \{ 2I(Z_1 < \Delta_1, Z_2 < \Delta_2) - 2I(Z_1 < \Delta_1)I(Z'_2 < \Delta_2) \} \\
&- \mathbb{E} \{ 2I(Z_1 < \Delta_1, Z_2 > \Delta_2, Z'_2 > \Delta_2) \text{sign}(Z_2 - Z'_2) \} \\
&- \mathbb{E} \{ 2I(Z_2 < \Delta_2, Z_1 > \Delta_1, Z'_1 > \Delta_1) \text{sign}(Z_1 - Z'_1) \} \\
&+ \mathbb{E} \{ I(Z_1 > \Delta_1, Z'_1 > \Delta_1, Z_2 > \Delta_2, Z'_2 > \Delta_2) \text{sign}(Z_1 - Z'_1) \text{sign}(Z_2 - Z'_2) \}.
\end{aligned}$$

Using  $\text{sign}(x) = I(x > 0) - I(x < 0)$  and (13), it holds that

$$\begin{aligned}\tau_{12} &= 2\Phi_2(\Delta_1, \Delta_2; \Sigma_{12}) - 2\Phi(\Delta_1)\Phi(\Delta_2) \\ &\quad - 2\mathbb{E}\{I(Z_1 < \Delta_1, Z'_2 > \Delta_2, Z_2 - Z'_2 > 0)\} + 2\mathbb{E}\{I(Z_1 < \Delta_1, Z_2 > \Delta_2, Z_2 - Z'_2 < 0)\} \\ &\quad - 2\mathbb{E}\{I(Z_2 < \Delta_2, Z'_1 > \Delta_1, Z_1 - Z'_1 > 0)\} + 2\mathbb{E}\{I(Z_2 < \Delta_2, Z_1 > \Delta_1, Z_1 - Z'_1 < 0)\} \\ &\quad + \mathbb{E}\{2I(Z_2 > \Delta_2, Z_1 > \Delta_1, Z_1 - Z'_1 < 0, Z_2 - Z'_2 < 0) \\ &\quad - 2I(Z'_1 > \Delta_1, Z_2 > \Delta_2, Z'_1 - Z_1 < 0, Z_2 - Z'_2 < 0)\}.\end{aligned}$$

Using the definition of the normal cumulative distribution function,  $\tau_{12}$  can be re-written as

$$\begin{aligned}\tau_{12} &= 2\Phi_2(\Delta_1, \Delta_2; \Sigma_{12}) - 2\Phi(\Delta_1)\Phi(\Delta_2) \\ &\quad - 2\Phi_3\left\{\Delta_1, -\Delta_2, 0; \begin{pmatrix} 1 & 0 & -\Sigma_{12}/\sqrt{2} \\ 0 & 1 & -1/\sqrt{2} \\ -\Sigma_{12}/\sqrt{2} & -1/\sqrt{2} & 1 \end{pmatrix}\right\} \\ &\quad + 2\Phi_3\left\{\Delta_1, -\Delta_2, 0; \begin{pmatrix} 1 & -\Sigma_{12} & \Sigma_{12}/\sqrt{2} \\ -\Sigma_{12} & 1 & -1/\sqrt{2} \\ \Sigma_{12}/\sqrt{2} & -1/\sqrt{2} & 1 \end{pmatrix}\right\} \\ &\quad - 2\Phi_3\left\{-\Delta_1, \Delta_2, 0; \begin{pmatrix} 1 & 0 & -1/\sqrt{2} \\ 0 & 1 & -\Sigma_{12}/\sqrt{2} \\ -1/\sqrt{2} & -\Sigma_{12}/\sqrt{2} & 1 \end{pmatrix}\right\} \\ &\quad + 2\Phi_3\left\{-\Delta_1, \Delta_2, 0; \begin{pmatrix} 1 & -\Sigma_{12} & -1/\sqrt{2} \\ -\Sigma_{12} & 1 & \Sigma_{12}/\sqrt{2} \\ -1/\sqrt{2} & \Sigma_{12}/\sqrt{2} & 1 \end{pmatrix}\right\} \\ &\quad + 2\Phi_4\left\{-\Delta_1, -\Delta_2, 0, 0; \begin{pmatrix} 1 & \Sigma_{12} & -1/\sqrt{2} & -\Sigma_{12}/\sqrt{2} \\ \Sigma_{12} & 1 & -\Sigma_{12}/\sqrt{2} & -1/\sqrt{2} \\ -1/\sqrt{2} & -\Sigma_{12}/\sqrt{2} & 1 & \Sigma_{12} \\ -\Sigma_{12}/\sqrt{2} & -1/\sqrt{2} & \Sigma_{12} & 1 \end{pmatrix}\right\} \\ &\quad - 2\Phi_4\left\{-\Delta_1, -\Delta_2, 0, 0; \begin{pmatrix} 1 & 0 & -1/\sqrt{2} & \Sigma_{12}/\sqrt{2} \\ 0 & 1 & \Sigma_{12}/\sqrt{2} & -1/\sqrt{2} \\ -1/\sqrt{2} & \Sigma_{12}/\sqrt{2} & 1 & -\Sigma_{12} \\ \Sigma_{12}/\sqrt{2} & -1/\sqrt{2} & -\Sigma_{12} & 1 \end{pmatrix}\right\}.\end{aligned}\tag{13}$$

Let the last six terms be denoted as  $T_1$  to  $T_6$  respectively. Then,

$$\tau_{12} = 2\Phi_2(\Delta_1, \Delta_2; \Sigma_{12}) - 2\Phi(\Delta_1)\Phi(\Delta_2) + T_1 + T_2 + T_3 + T_4 + T_5 + T_6.$$

Now we consider each separately, simplify using the (12)-type trick for 3 and 4-dimension of normal cdf  $\Phi_3(\cdot, \cdot, \cdot; r)$ ,  $\Phi_4(\cdot, \cdot, \cdot, \cdot; r)$  and we will combine them at the end.

$$\begin{aligned}T_3 + T_4 &= 2\Phi_3\left\{-\Delta_1, -\Delta_2, 0; \begin{pmatrix} 1 & 0 & -1/\sqrt{2} \\ 0 & 1 & \Sigma_{12}/\sqrt{2} \\ -1/\sqrt{2} & \Sigma_{12}/\sqrt{2} & 1 \end{pmatrix}\right\} \\ &\quad - 2\Phi_3\left\{-\Delta_1, -\Delta_2, 0; \begin{pmatrix} 1 & \Sigma_{12} & -1/\sqrt{2} \\ \Sigma_{12} & 1 & -\Sigma_{12}/\sqrt{2} \\ -1/\sqrt{2} & -\Sigma_{12}/\sqrt{2} & 1 \end{pmatrix}\right\} \\ &= T'_3 + T'_4\end{aligned}\tag{14}$$

$$\begin{aligned}
T'_4 + T_5 &= -2\Phi_4 \left\{ -\Delta_1, -\Delta_2, 0, 0; \begin{pmatrix} 1 & \Sigma_{12} & -1/\sqrt{2} & \Sigma_{12}/\sqrt{2} \\ \Sigma_{12} & 1 & -\Sigma_{12}/\sqrt{2} & 1/\sqrt{2} \\ -1/\sqrt{2} & -\Sigma_{12}/\sqrt{2} & 1 & -\Sigma_{12} \\ \Sigma_{12}/\sqrt{2} & 1/\sqrt{2} & -\Sigma_{12} & 1 \end{pmatrix} \right\}; \\
T'_3 + T_6 &= 2\Phi_4 \left\{ -\Delta_1, -\Delta_2, 0, 0; \begin{pmatrix} 1 & 0 & -1/\sqrt{2} & -\Sigma_{12}/\sqrt{2} \\ 0 & 1 & \Sigma_{12}/\sqrt{2} & 1/\sqrt{2} \\ -1/\sqrt{2} & \Sigma_{12}/\sqrt{2} & 1 & \Sigma_{12} \\ -\Sigma_{12}/\sqrt{2} & 1/\sqrt{2} & \Sigma_{12} & 1 \end{pmatrix} \right\}. \\
T_1 + T_2 &= 2\Phi_3 \left\{ -\Delta_1, -\Delta_2, 0; \begin{pmatrix} 1 & 0 & \Sigma_{12}/\sqrt{2} \\ 0 & 1 & -1/\sqrt{2} \\ \Sigma_{12}/\sqrt{2} & -1/\sqrt{2} & 1 \end{pmatrix} \right\} \\
&\quad - 2\Phi_3 \left\{ -\Delta_1, -\Delta_2, 0; \begin{pmatrix} 1 & \Sigma_{12} & -\Sigma_{12}/\sqrt{2} \\ \Sigma_{12} & 1 & -1/\sqrt{2} \\ -\Sigma_{12}/\sqrt{2} & -1/\sqrt{2} & 1 \end{pmatrix} \right\}.
\end{aligned}$$

Applying the (12)-type trick one more time yields

$$\begin{aligned}
T_1 + T_2 &= 2\Phi_2(-\Delta_1, -\Delta_2; 0) - 2\Phi_3 \left\{ -\Delta_1, -\Delta_2, 0; \begin{pmatrix} 1 & 0 & -\Sigma_{12}/\sqrt{2} \\ 0 & 1 & -1/\sqrt{2} \\ -\Sigma_{12}/\sqrt{2} & -1/\sqrt{2} & 1 \end{pmatrix} \right\} \\
&\quad - 2\Phi_2(-\Delta_1, -\Delta_2; \Sigma_{12}) + 2\Phi_3 \left\{ -\Delta_1, -\Delta_2, 0; \begin{pmatrix} 1 & \Sigma_{12} & \Sigma_{12}/\sqrt{2} \\ \Sigma_{12} & 1 & 1/\sqrt{2} \\ \Sigma_{12}/\sqrt{2} & 1/\sqrt{2} & 1 \end{pmatrix} \right\} \\
&= 2\Phi_2(-\Delta_1, -\Delta_2; 0) - 2\Phi_2(-\Delta_1, -\Delta_2; \Sigma_{12}) + T'_1 + T'_2
\end{aligned}$$

The first terms in the previous display are cancelled out with the first two terms in (14) because

$$\begin{aligned}
2\Phi_2(-\Delta_1, -\Delta_2; 0) &= 2 - 2\Phi(\Delta_1) - 2\Phi(\Delta_2) + 2\Phi(\Delta_1)\Phi(\Delta_2) \\
-2\Phi_2(-\Delta_1, -\Delta_2; \Sigma_{12}) &= 2\Phi(\Delta_1) + 2\Phi(\Delta_2) - 2 - 2\Phi_2(\Delta_1, \Delta_2; \Sigma_{12}).
\end{aligned}$$

Furthermore,  $T'_1$  and  $T'_3 + T_6$ ,  $T'_2$  and  $T'_4 + T_5$  can be combined into one term, respectively.

$$\begin{aligned}
T'_1 + (T'_3 + T_6) &= -2\Phi_4 \left\{ -\Delta_1, -\Delta_2, 0, 0; \begin{pmatrix} 1 & 0 & 1/\sqrt{2} & -\Sigma_{12}/\sqrt{2} \\ 0 & 1 & -\Sigma_{12}/\sqrt{2} & 1/\sqrt{2} \\ 1/\sqrt{2} & -\Sigma_{12}/\sqrt{2} & 1 & -\Sigma_{12} \\ -\Sigma_{12}/\sqrt{2} & 1/\sqrt{2} & -\Sigma_{12} & 1 \end{pmatrix} \right\} \\
T'_2 + (T'_4 + T_5) &= 2\Phi_4 \left\{ -\Delta_1, -\Delta_2, 0, 0; \begin{pmatrix} 1 & \Sigma_{12} & 1/\sqrt{2} & \Sigma_{12}/\sqrt{2} \\ \Sigma_{12} & 1 & \Sigma_{12}/\sqrt{2} & 1/\sqrt{2} \\ 1/\sqrt{2} & \Sigma_{12}/\sqrt{2} & 1 & \Sigma_{12} \\ \Sigma_{12}/\sqrt{2} & 1/\sqrt{2} & \Sigma_{12} & 1 \end{pmatrix} \right\}
\end{aligned}$$

This concludes the proof of Theorem 4. □

**Lemma 1.** For any constants  $a_1, \dots, a_d$ , let  $\Phi_d(a_1, \dots, a_d; \Sigma_d(t))$  be the cumulative distribution function of  $d$ -dimensional central normal distribution with covariance matrix

$$\Sigma_d(t) = \begin{pmatrix} 1 & \rho_{12}(t) & \rho_{13}(t) & \cdots & \rho_{1d}(t) \\ \rho_{21}(t) & 1 & \rho_{23}(t) & \cdots & \rho_{2d}(t) \\ & & 1 & & \\ \vdots & & & \ddots & \vdots \\ \rho_{d1}(t) & & \cdots & & 1 \end{pmatrix}.$$

Then there exist  $h_{ij}(t) > 0$  for all  $t \in (-1, 1)$  such that

$$\frac{\partial \Phi_d(a_1, \dots, a_d; \Sigma_d(t))}{\partial t} = \sum_{i=1}^{d-1} \sum_{j=i+1}^d h_{ij}(t) \frac{\partial \rho_{ij}(t)}{\partial t}.$$

**Proof of Lemma 1.** Using the multivariate chain rule,

$$\frac{\partial \Phi_d(a_1, \dots, a_d; \Sigma_d(t))}{\partial t} = \sum_{i < j} \left\{ \frac{\partial \Phi_d(a_1, \dots, a_d; \Sigma_d(t))}{\partial \rho_{ij}(t)} \frac{\partial \rho_{ij}(t)}{\partial t} \right\} := \sum_{i < j} h_{ij}(t) \frac{\partial \rho_{ij}(t)}{\partial t}.$$

Without loss of generality, let  $i = 1, j = 2$  and consider  $h_{12}(t)$ . By dominated convergence theorem, we can interchange integration and differentiation to get

$$\begin{aligned} \frac{\partial \Phi_d(a_1, \dots, a_d; \Sigma_d(t))}{\partial \rho_{12}(t)} &= \int_{-\infty}^{a_1} \cdots \int_{-\infty}^{a_d} \frac{\partial \phi_d(x_1, x_2, x_3, \dots, x_d; \Sigma_d(t))}{\partial \rho_{12}(t)} dx_d \cdots dx_3 dx_2 dx_1 \\ &= \int_{-\infty}^{a_3} \cdots \int_{-\infty}^{a_d} \int_{-\infty}^{a_1} \int_{-\infty}^{a_2} \frac{\partial^2 \phi_d(x_1, x_2, x_3, \dots, x_d; \Sigma_d(t))}{\partial x_1 \partial x_2} dx_2 dx_1 dx_d \cdots dx_3 \\ &= \int_{-\infty}^{a_3} \cdots \int_{-\infty}^{a_d} \phi_d(a_1, a_2, x_3, \dots, x_d; \Sigma_d(t)) dx_d \cdots dx_3, \end{aligned}$$

where in the 2nd equality we used  $\partial \phi_d / \partial \rho_{ij} = \partial^2 \phi_d / (\partial x_i \partial x_j)$  (Plackett, 1954). Since  $\phi$  is multivariate density function,  $h_{12}(t) = \partial \Phi_d(a_1, \dots, a_d; \Sigma_d(t)) / \partial \rho_{12}(t)$  is positive. The proof for other  $i, j$  is analogous.  $\square$

**Proof of Theorem 5.** Let  $\Sigma_{jk} = t$ . We consider separately each of the three cases.

1) For the truncated/binary case, the bridge function (Theorem 2) has the form

$$F(t; \Delta_j, \Delta_k) = 2\{1 - \Phi(\Delta_j)\}\Phi(\Delta_k) - 2\Phi_3(-\Delta_j, \Delta_k, 0; \Sigma_{3a}(t)) - 2\Phi_3(-\Delta_j, \Delta_k, 0; \Sigma_{3b}(t)),$$

where

$$\Sigma_{3a}(t) = \begin{pmatrix} 1 & -t & 1/\sqrt{2} \\ -t & 1 & -t/\sqrt{2} \\ 1/\sqrt{2} & -t/\sqrt{2} & 1 \end{pmatrix}, \quad \Sigma_{3b}(t) = \begin{pmatrix} 1 & 0 & -1/\sqrt{2} \\ 0 & 1 & -t/\sqrt{2} \\ -1/\sqrt{2} & -t/\sqrt{2} & 1 \end{pmatrix}.$$

From Lemma 1,

$$\begin{aligned} \frac{\partial \Phi_3(-\Delta_j, \Delta_k, 0; \Sigma_{3a}(t))}{\partial t} &= \sum_{i=1}^2 \sum_{i'=i+1}^3 h_{ii'}(t) \frac{\partial \rho_{ii'}(t)}{\partial t} \\ &= h_{12}(t)(-1) + h_{13}(t)(0) + h_{23}(t)(-1/\sqrt{2}) < 0, \end{aligned}$$



and similarly

$$\frac{\partial \Phi_3(-\Delta_j, \Delta_k, 0; \Sigma_{3b}(t))}{\partial t} = h_{23}(t)(-1/\sqrt{2}) < 0.$$

Therefore,

$$\frac{\partial F(t; \Delta_j, \Delta_k)}{\partial t} = -2 \frac{\partial \Phi_3(-\Delta_j, \Delta_k, 0; \Sigma_{3a}(t))}{\partial t} - 2 \frac{\partial \Phi_3(-\Delta_j, \Delta_k, 0; \Sigma_{3b}(t))}{\partial t} > 0.$$

It follows that  $F(t; \Delta_j, \Delta_k)$  is increasing in  $t$ .

2) For the truncated/continuous case, the bridge function (Theorem 3) has the form

$$F(t; \Delta_j) = -2\Phi_2(-\Delta_j, 0; 1/\sqrt{2}) + 4\Phi_3(-\Delta_j, 0, 0; \Sigma_3(t)),$$

with

$$\Sigma_3(t) = \begin{pmatrix} 1 & 1/\sqrt{2} & t/\sqrt{2} \\ 1/\sqrt{2} & 1 & t \\ t/\sqrt{2} & t & 1 \end{pmatrix}.$$

Using Lemma 1,

$$\frac{\partial \Phi_3(-\Delta_j, 0, 0; \Sigma_3(t))}{\partial t} = \sum_{i=1}^2 \sum_{i'=i+1}^3 h_{ii'}(t) \frac{\partial \rho_{ii'}(t)}{\partial t} = h_{12}(t)(0) + h_{13}(t)(1/\sqrt{2}) + h_{23}(t)(1) > 0.$$

Thus,

$$\frac{\partial F(t; \Delta_j)}{\partial t} = 4 \frac{\partial \Phi_3(-\Delta_j, 0, 0; \Sigma_3(t))}{\partial t} > 0,$$

which implies that  $F(t; \Delta_j)$  is increasing in  $t$ .

3) For the truncated/binary case, the bridge function (Theorem 4) has the form

$$F(t; \Delta_j, \Delta_k) = -2\Phi_4(-\Delta_j, -\Delta_k, 0, 0; \Sigma_{4a}(t)) + 2\Phi_4(-\Delta_j, -\Delta_k, 0, 0; \Sigma_{4b}(t)),$$

$$\Sigma_{4a}(t) = \begin{pmatrix} 1 & 0 & 1/\sqrt{2} & -t/\sqrt{2} \\ 0 & 1 & -t/\sqrt{2} & 1/\sqrt{2} \\ 1/\sqrt{2} & -t/\sqrt{2} & 1 & -t \\ -t/\sqrt{2} & 1/\sqrt{2} & -t & 1 \end{pmatrix}, \quad \Sigma_{4b}(t) = \begin{pmatrix} 1 & t & 1/\sqrt{2} & t/\sqrt{2} \\ t & 1 & t/\sqrt{2} & 1/\sqrt{2} \\ 1/\sqrt{2} & t/\sqrt{2} & 1 & t \\ t/\sqrt{2} & 1/\sqrt{2} & t & 1 \end{pmatrix}.$$

From Lemma 1,

$$\begin{aligned} \frac{\partial \Phi_4(-\Delta_j, -\Delta_k, 0, 0; \Sigma_{4a}(t))}{\partial t} &= \sum_{i=1}^3 \sum_{i'=i+1}^4 h_{ii'}(t) \frac{\partial \rho_{ii'}(t)}{\partial t} \\ &= h_{14}(t)(-1/\sqrt{2}) + h_{23}(t)(-1/\sqrt{2}) + h_{34}(t)(-1) < 0, \end{aligned}$$

and similarly

$$\frac{\partial \Phi_4(-\Delta_j, -\Delta_k, 0, 0; \Sigma_{4b}(t))}{\partial t} = h_{12}(t)(1) + h_{14}(t)(1/\sqrt{2}) + h_{23}(t)(1/\sqrt{2}) + h_{34}(t)(1) > 0.$$

Therefore,

$$\frac{\partial F(t; \Delta_j, \Delta_k)}{\partial t} = -2 \frac{\partial \Phi_4(-\Delta_j, -\Delta_k, 0, 0; \Sigma_{4a}(t))}{\partial t} + 2 \frac{\partial \Phi_4(-\Delta_j, -\Delta_k, 0, 0; \Sigma_{4b}(t))}{\partial t} > 0.$$

Thus, all bridge functions are strictly increasing with  $t$ .

□

**Proof of Proposition 1.** This proof follows the proof of Proposition 2 in [Witten and Tibshirani \(2011\)](#). Consider the Karush-Kuhn-Tucker (KKT) conditions for problem (5):

$$\begin{aligned} \text{Lagrangian condition: } & -\tilde{R}_{12}w_2 + \lambda_1 z + 2\mu\tilde{R}_1w_1 = 0; \\ \text{Complementary slackness: } & \mu(w_1^\top \tilde{R}_1w_1 - 1) = 0; \\ \text{Primal/dual feasibility: } & \mu \geq 0, \quad w_1^\top \tilde{R}_1w_1 - 1 \leq 0; \end{aligned}$$

where  $z$  is the subgradient of  $\|w_1\|_1$ , i.e.  $z_j = \text{sign}(w_{1j})$  if  $w_{1j} \neq 0$  and  $z_j \in [-1, 1]$  if  $w_{1j} = 0$ .

First, if  $w_1 = 0$ , then we must have  $\mu = 0$  and  $-(\tilde{R}_{12}w_2)_j + \lambda_1 z_j = 0$  should hold for all  $j$ . This is only possible when  $z_j = (\tilde{R}_{12}w_2)_j / \lambda_1 \in [-1, 1]$  for all  $j$ , that is  $\|\tilde{R}_{12}w_2\|_\infty \leq \lambda_1$ . Therefore, if  $\|\tilde{R}_{12}w_2\|_\infty \leq \lambda_1$ , then  $w_1 = 0$  solves (5). For problem (6), since  $-\tilde{R}_{12}w_2 + \lambda_1 z + \tilde{R}_1w_1 = 0$  where  $z$  is the subgradient vector of  $\|w_1\|_1$ ,  $w_1 = 0$  solves problem (6) and if  $\hat{w}_1 = 0$ , then  $w_1 = 0$ .

Second, if we suppose instead that  $\|\tilde{R}_{12}w_2\|_\infty > \lambda_1$ , then  $w_1 \neq 0$  and  $w_1^\top \tilde{R}_1w_1 = 1$  should be the case, which now simplifies conditions to

$$-\tilde{R}_{12}w_2 + \lambda_1 z + 2\mu\tilde{R}_1w_1 = 0; \quad w_1^\top \tilde{R}_1w_1 = 1; \quad \mu > 0.$$

If we let  $\tilde{w}_1 = 2\mu w_1$ , then this is equivalent to solving problem (6) and then dividing the solution by  $(w_1^\top \tilde{R}_1\tilde{w}_1)^{1/2}$ .  $\square$

## Appendix B Additional simulation results

Figures 6–11 display additional simulation results for the truncated/binary and truncated/continuous cases. For truncated/binary case, the method of [Witten and Tibshirani \(2009\)](#) has comparable or better prediction performance than both variations of our approach; however, it has worse variable selection performance due to significantly larger support sizes for both canonical vectors. For truncated/continuous case, the conclusions are qualitatively similar to Section 4 with our method having the best overall prediction performance with BIC2 criterion, and best variable selection performance with BIC1 criterion.

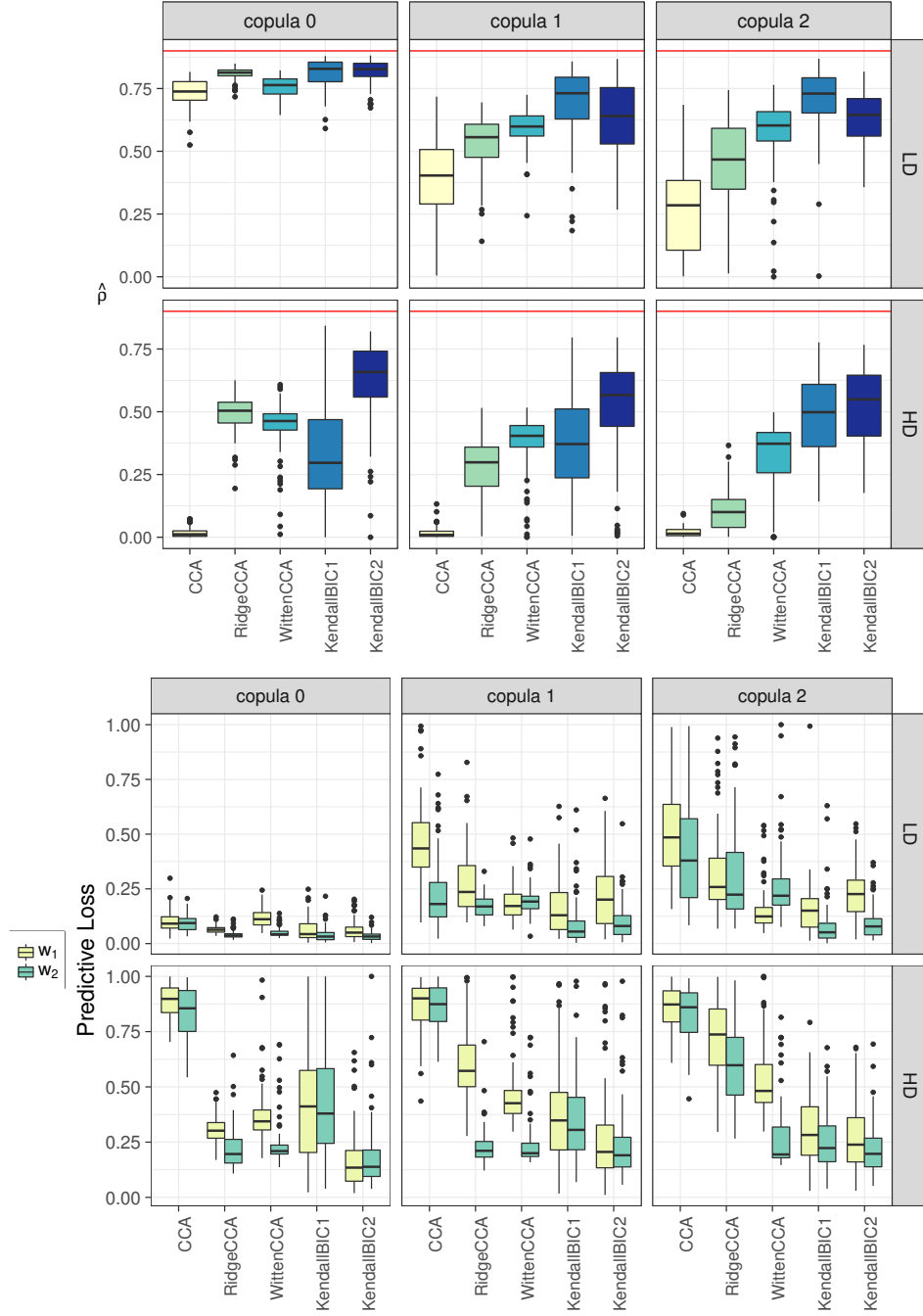


Figure 6: Truncated/continuous case. **Top:** The value of  $\hat{\rho}$  from (7). The horizontal lines indicate the true canonical correlation value  $\rho = 0.9$ . **Bottom:** The value of predictive loss (8). Results over 100 replications. CCA: Sample canonical correlation analysis; RidgeCCA: Canonical ridge of González et al. (2008); WittenCCA: method of Witten et al. (2009); KendallBIC1, KendallBIC2: proposed method with tuning parameter selected using either BIC1 or BIC2 criterion; LD: low-dimensional setting ( $p_1 = p_2 = 25$ ); HD: high-dimensional setting ( $p_1 = p_2 = 100$ ).

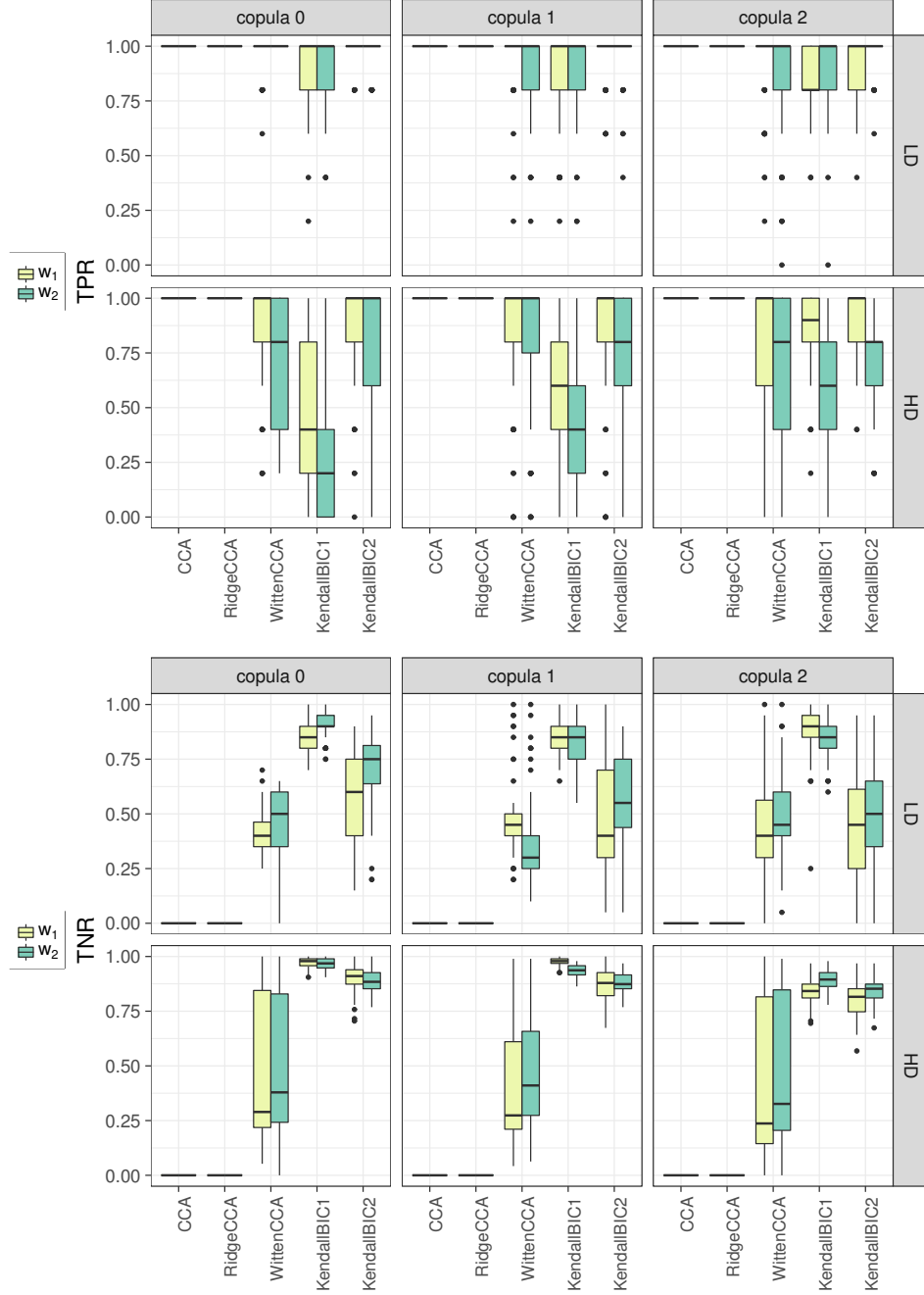


Figure 7: Truncated/continuous case. **Top:** True positive rate (TPR); **Bottom:** True negative rate (TNR). Results over 100 replications. CCA: Sample canonical correlation analysis; RidgeCCA: Canonical Ridge of [González et al. \(2008\)](#); WittenCCA: method of [Witten et al. \(2009\)](#); KendallBIC1, KendallBIC2: proposed method with tuning parameter selected using either BIC1 or BIC2 criterion; LD: low-dimensional setting ( $p_1 = p_2 = 25$ ); HD: high-dimensional setting ( $p_1 = p_2 = 100$ ).

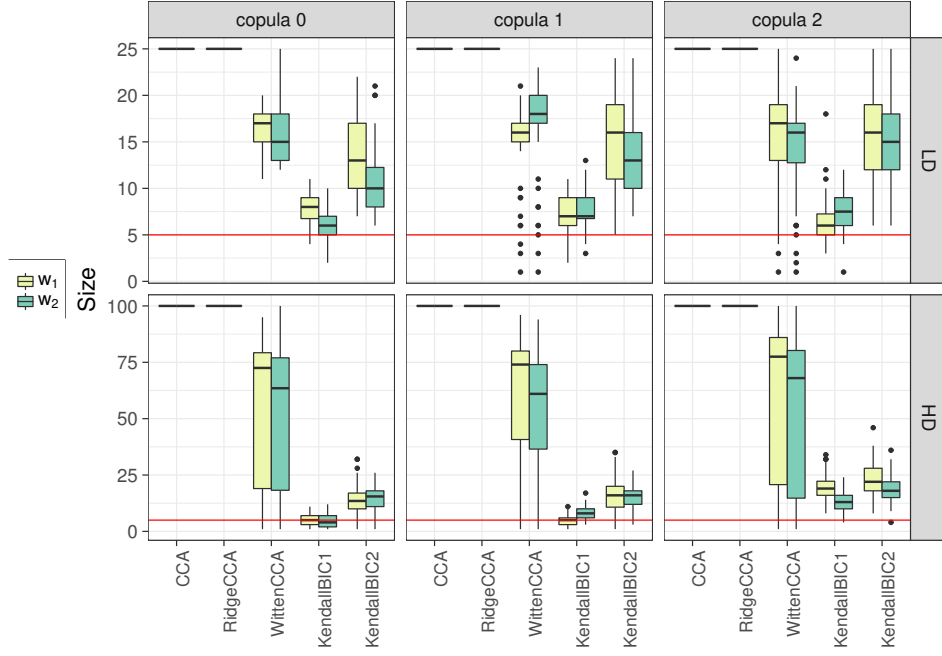


Figure 8: Truncated/continuous case. Selected model size over 100 replications. The horizontal lines indicate the true model size 5. CCA: Sample canonical correlation analysis; RidgeCCA: Canonical Ridge of [González et al. \(2008\)](#); WittenCCA: method of [Witten et al. \(2009\)](#); KendallBIC1, KendallBIC2: proposed method with tuning parameter selected using either BIC1 or BIC2 criterion; LD: low-dimensional setting ( $p_1 = p_2 = 25$ ); HD: high-dimensional setting ( $p_1 = p_2 = 100$ ).

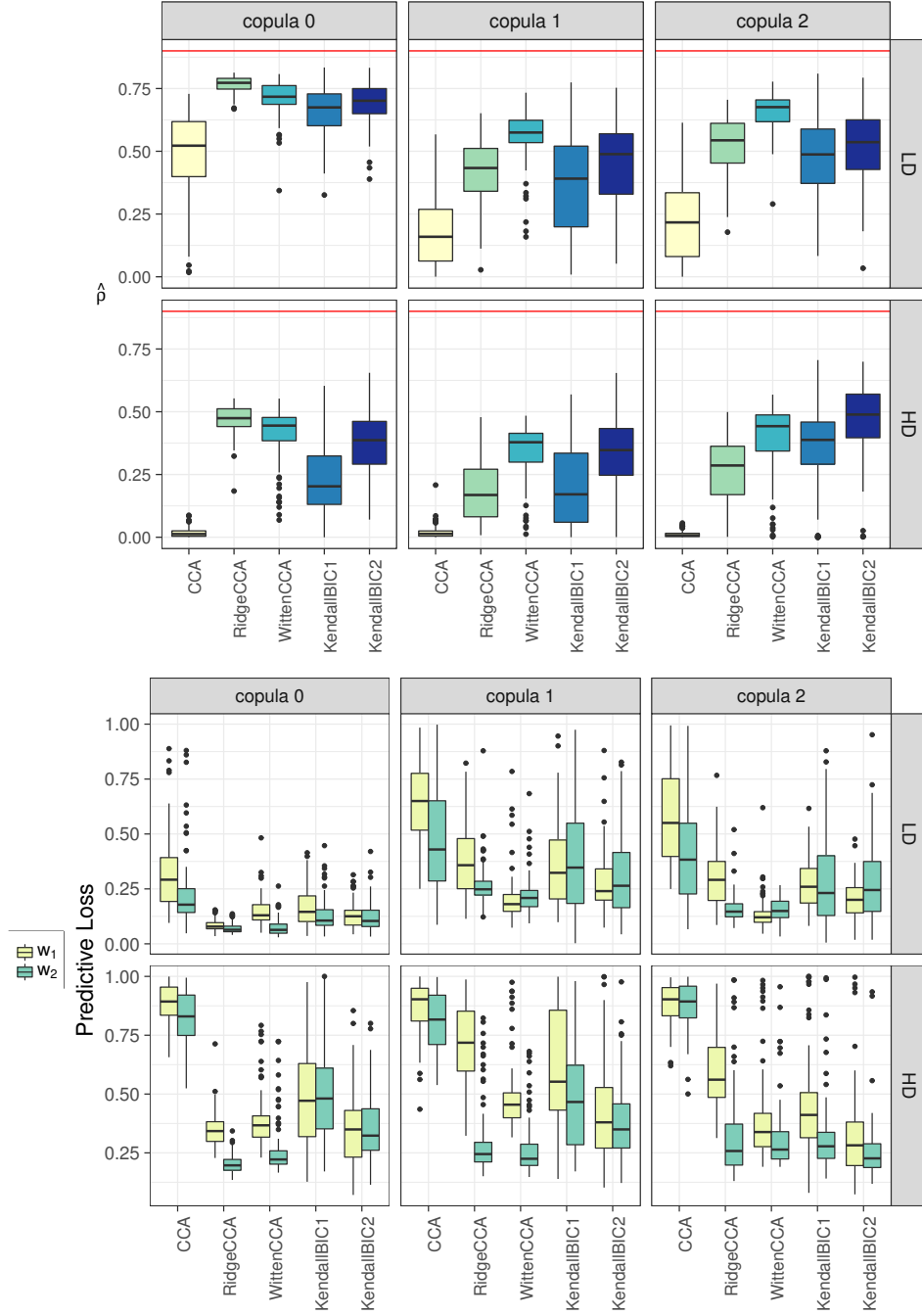


Figure 9: Truncated/binary case. **Top:** The value of  $\hat{\rho}$  from (7). The horizontal lines indicate the true canonical correlation value  $\rho = 0.9$ . **Bottom:** The value of predictive loss (8). Results over 100 replications. CCA: Sample canonical correlation analysis; RidgeCCA: Canonical ridge of González et al. (2008); WittenCCA: method of Witten et al. (2009); KendallBIC1, KendallBIC2: proposed method with tuning parameter selected using either BIC1 or BIC2 criterion; LD: low-dimensional setting ( $p_1 = p_2 = 25$ ); HD: high-dimensional setting ( $p_1 = p_2 = 100$ ).

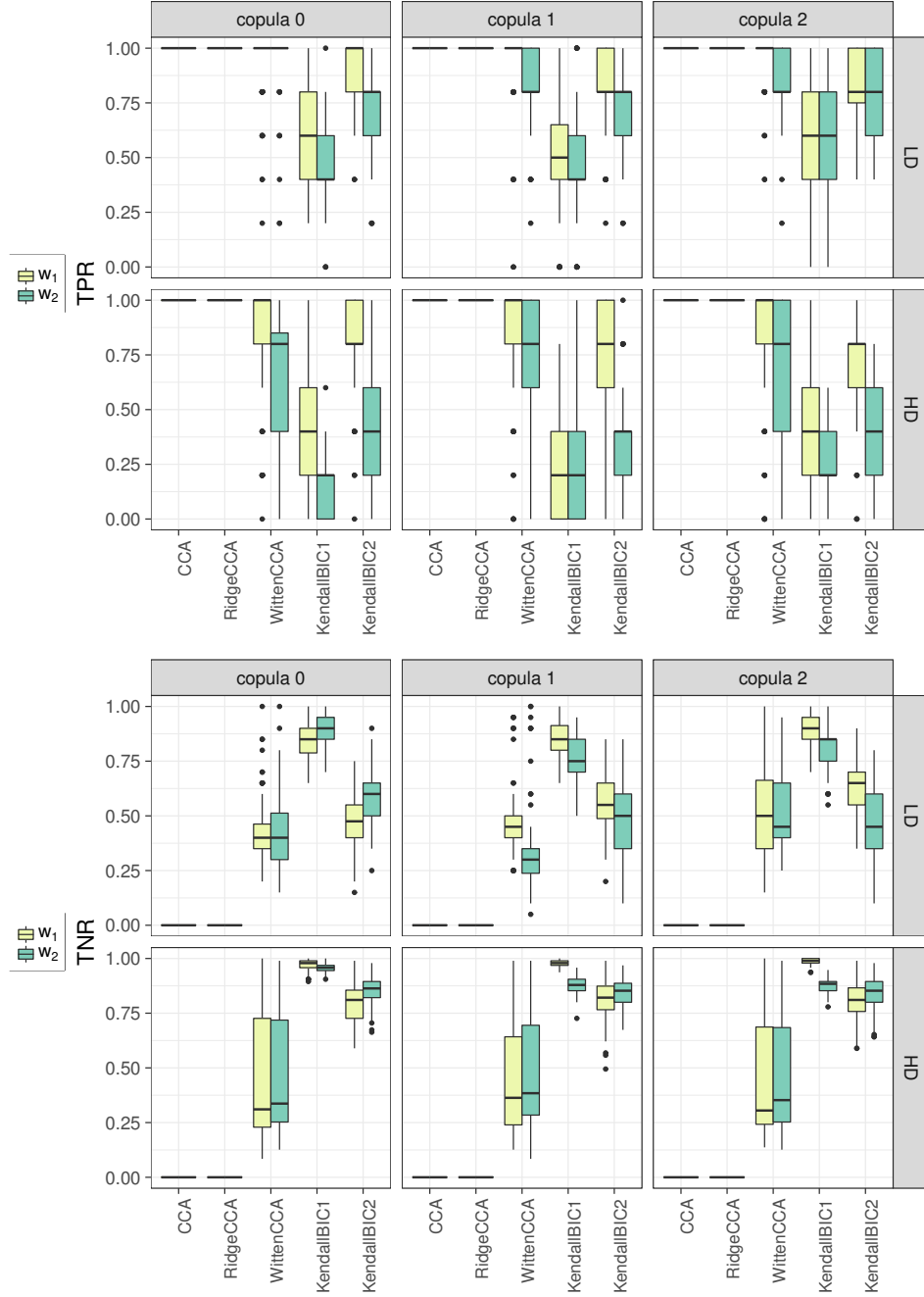


Figure 10: Truncated/binary case. **Top:** True positive rate (TPR); **Bottom:** True negative rate (TNR). Results over 100 replications. CCA: Sample canonical correlation analysis; RidgeCCA: Canonical Ridge of [González et al. \(2008\)](#); WittenCCA: method of [Witten et al. \(2009\)](#); Kendall-BIC1, KendallBIC2: proposed method with tuning parameter selected using either BIC1 or BIC2 criterion; LD: low-dimensional setting ( $p_1 = p_2 = 25$ ); HD: high-dimensional setting ( $p_1 = p_2 = 100$ ).



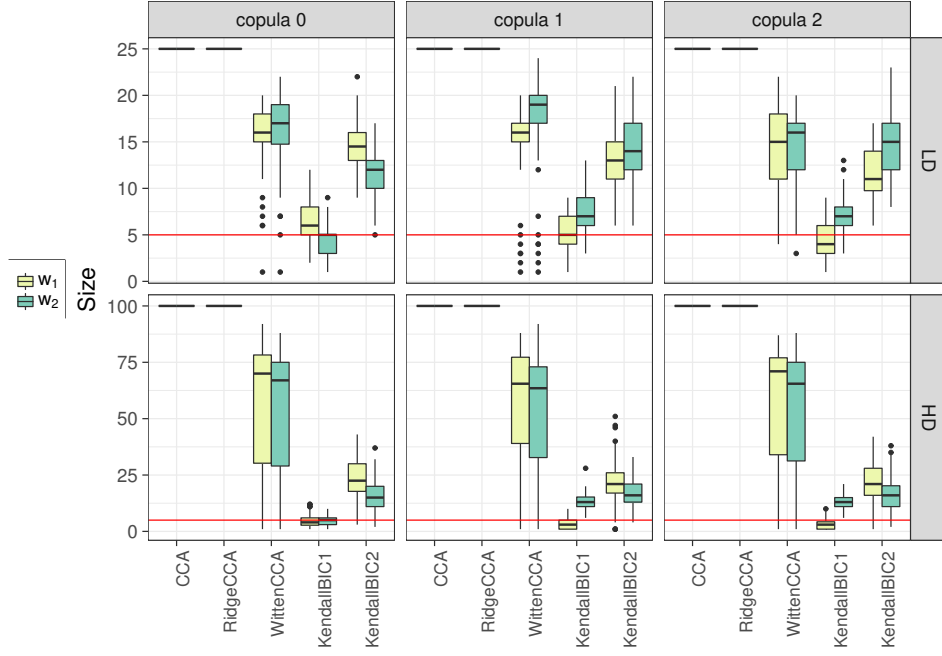


Figure 11: Truncated/binary case. Selected model size over 100 replications. The horizontal lines indicate the true model size 5. CCA: Sample canonical correlation analysis; RidgeCCA: Canonical Ridge of [González et al. \(2008\)](#); WittenCCA: method of [Witten et al. \(2009\)](#); KendallBIC1, KendallBIC2: proposed method with tuning parameter selected using either BIC1 or BIC2 criterion; LD: low-dimensional setting ( $p_1 = p_2 = 25$ ); HD: high-dimensional setting ( $p_1 = p_2 = 100$ ).

## References

- Aakula, A., Leivonen, S.-K., Hintsanen, P., Aittokallio, T., Ceder, Y., Børresen-Dale, A.-L., Perälä, M., Östling, P., and Kallioniemi, O. (2015). MicroRNA-135b regulates ER $\alpha$ , AR and HIF1AN and affects breast and prostate cancer cell growth. *Molecular Oncology*, 9, 1287–1300.
- Agniel, D. and Cai, T. (2017). Analysis of multiple diverse phenotypes via semiparametric canonical correlation analysis. *Biometrics*, 73, 1254–1265.
- Bach, F. R. and Jordan, M. I. (2005). A probabilistic interpretation of canonical correlation analysis. Technical Report 688, Department of Statistics, University of California, Berkeley.
- Boyd, S. P. and Vandenberghe, L. (2004). *Convex Optimization*. Cambridge Univ Press, Cambridge.
- Chen, M., Gao, C., Ren, Z., and Zhou, H. H. (2013). Sparse CCA via precision adjusted iterative thresholding. *arXiv*, page 1311.6186v1.
- Chi, E. C., Allen, G. I., Zhou, H., Kohannim, O., Lange, K., and Thompson, P. M. (2013). Imaging genetics via sparse canonical correlation analysis. In *2013 IEEE 10th International Symposium on Biomedical Imaging*, pages 740–743.
- Cruz-Cano, R. and Lee, M.-L. T. (2014). Fast regularized canonical correlation analysis. *Computational Statistics & Data Analysis*, 70, 88–100.
- Fan, J., Liu, H., Ning, Y., and Zou, H. (2017). High dimensional semiparametric latent graphical model for mixed data. *J. R. Statist. Soc. B*, 79, 405–421.
- Gao, C., Ma, Z., and Zhou, H. H. (2017). Sparse CCA: Adaptive estimation and computational barriers. *Annals of Statistics*, 45, 2074–2101.
- González, I., Déjean, S., Martin, P. G., and Baccini, A. (2008). CCA: An R package to extend canonical correlation analysis. *Journal of Statistical Software*, 23, 1–14.
- Gorski, J., Pfeuffer, F., and Klamroth, K. (2007). Biconvex sets and optimization with biconvex functions: a survey and extensions. *Mathematical Methods of Operations Research*, 66, 373–407.
- Guo, Y., Ding, X., Liu, C., and Xue, J.-H. (2016). Sufficient canonical correlation analysis. *IEEE Transactions on Image Processing*, 25, 2610–2619.
- Hardoon, D. R., Szedmak, S., and Shawe-Taylor, J. (2004). Canonical correlation analysis: An overview with application to learning methods. *Neural Computation*, 16, 2639–2664.
- Hotelling, H. (1936). Relations between two sets of variates. *Biometrika*, 28, 321–377.
- Hu, D. G., Selth, L. A., Tarulli, G. A., Meech, R., Wijayakumara, D., Chanawong, A., Russell, R., Caldas, C., Robinson, J. L., Carroll, J. S., et al. (2016). Androgen and estrogen receptors in breast cancer coregulate human UDP-glucuronosyltransferases 2B15 and 2B17. *Cancer Research*, 76, 5881–5893.
- Hua, K., Jin, J., Zhao, J., Song, J., Song, H., Li, D., Maskey, N., Zhao, B., Wu, C., Xu, H., et al. (2016). miR-135b, upregulated in breast cancer, promotes cell growth and disrupts the cell cycle by regulating LATS2. *International Journal of Oncology*, 48, 1997–2006.

- Kim, J.-Y., Jung, H. H., Do, I.-G., Bae, S., Lee, S. K., Kim, S. W., Lee, J. E., Nam, S. J., Ahn, J. S., Park, Y. H., et al. (2016). Prognostic value of ERBB4 expression in patients with triple negative breast cancer. *BMC Cancer*, 16, 138.
- Liu, H., Lafferty, J., and Wasserman, L. (2009). The nonparanormal: Semiparametric estimation of high dimensional undirected graphs. *Journal of Machine Learning Research*, 10, 2295–2328.
- Manvati, S., Mangalhara, K. C., Kalaiarasan, P., Srivastava, N., and Bamezai, R. (2015). miR-24-2 regulates genes in survival pathway and demonstrates potential in reducing cellular viability in combination with docetaxel. *Gene*, 567, 217–224.
- Parkhomenko, E., Tritchler, D., and Beyene, J. (2009). Sparse canonical correlation analysis with application to genomic data integration. *Statistical Applications in Genetics and Molecular Biology*, 8, 1–34.
- Piggin, C. L., Roden, D. L., Gallego-Ortega, D., Lee, H. J., Oakes, S. R., and Ormandy, C. J. (2016). ELF5 isoform expression is tissue-specific and significantly altered in cancer. *Breast Cancer Research*, 18, 4.
- Plackett, R. L. (1954). A reduction formula for normal multivariate integrals. *Biometrika*, 41, 351–360.
- Reid, S., Tibshirani, R., and Friedman, J. (2016). A study of error variance estimation in lasso regression. *Statistica Sinica*, 26, 35–67.
- Safo, S. E., Li, S., and Long, Q. (2018). Integrative analysis of transcriptomic and metabolomic data via sparse canonical correlation analysis with incorporation of biological information. *Biometrics*, 74, 300–312.
- Tibshirani, R. (1996). Regression shrinkage and selection via the lasso. *J. R. Statist. Soc. B*, 58, 267–288.
- Tibshirani, R. J. and Taylor, J. (2012). Degrees of freedom in lasso problems. *Annals of Statistics*, 40, 1198–1232.
- Tseng, P. (1988). Coordinate ascent for maximizing nondifferentiable concave functions. Technical report, Massachusetts Institute of Technology, Laboratory for Information and Decision Systems.
- Wilms, I. and Croux, C. (2015). Sparse canonical correlation analysis from a predictive point of view. *Biometrical Journal*, 57, 834–851.
- Witten, D. M. and Tibshirani, R. J. (2009). Extensions of sparse canonical correlation analysis with applications to genomic data. *Statistical Applications in Genetics and Molecular Biology*, 8, 1–27.
- Witten, D. M. and Tibshirani, R. J. (2011). Penalized classification using Fisher’s linear discriminant. *J. R. Statist. Soc. B*, 73, 753–772.
- Witten, D. M., Tibshirani, R. J., and Hastie, T. (2009). A penalized matrix decomposition, with applications to sparse principal components and canonical correlation analysis. *Biostatistics*, 10, 515–534.

- Xiao, B., Zhang, W., Chen, L., Hang, J., Wang, L., Zhang, R., Liao, Y., Chen, J., Ma, Q., Sun, Z., et al. (2018). Analysis of the miRNA–mRNA–lncRNA network in human estrogen receptor-positive and estrogen receptor-negative breast cancer based on TCGA data. *Gene*, 658, 28–35.
- Zoh, R. S., Mallick, B., Ivanov, I., Baladandayuthapani, V., Manyam, G., Chapkin, R. S., Lampe, J. W., and Carroll, R. J. (2016). PCAN: Probabilistic correlation analysis of two non-normal data sets. *Biometrics*, 72, 1358–1368.